7 OCT 1948

# NATIONAL ADVISORY COMMITTEE FOR AERONAUTICS

TECHNICAL NOTE

No. 1451

AN INVESTIGATION OF AIRCRAFT HEATERS

XXVII - DISTRIBUTION OF HEAT-TRANSFER RATE

IN THE ENTRANCE SECTION OF A CIRCULAR TUBE

By L. M. K. Boelter, G. Young, and H. W. Iversen

University of California

Washington

July 1948

FOR REFERENCE

TECHNICAL NOTE NO. 1451

# AN INVESTIGATION OF AIRCRAFT HEATERS

## XXVII — DISTRIBUTION OF HEAT-TRANSFER RATE

## IN THE ENTRANCE SECTION OF A CIRCULAR TUBE

By L. M. K. Boelter, G. Young, and H. W. Iversen

## SUMMARY

Experimental data on the variation of the point unit thermal conductance in the entrance section of a circular tube are presented for 16 different flow conditions of the entering air. Results are compared with values calculated from existing analytical solutions.

The average (integrated mean with length) unit thermal conductance is also calculated for eight entering-air conditions and is compared with values resulting from analytical methods. In many cases the experimental values are appreciably higher than those derived from equations which are based on over-all data taken on long pipes.

## INTRODUCTION

The present investigation was conducted to determine the distribution of heat-transfer rate resulting from a variation of the unit thermal conductance at the entrance to a tube for various conditions of the entering fluid.

Heretofore experimental data for the unit thermal conductance $f_c$ $\left(\text{in the equation } q = f_c A \left(t_w - t_a\right)\right)$ have been obtained as an average over the tube length. Equations for the determination of $f_c$ have usually been expressed in terms of the fluid properties and some fixed physical dimension of the system, such as the tube diameter. In many cases, when it is more important to know the value of the temperature at the particular point along the heat-transfer surface than to know the over-all rate of heat transfer, an average value of the unit thermal conductance $f_c$ is inadequate and the local value $f_{c_x}$ must be determined. The equations for the unit thermal conductance should then be expressed in terms of a variable physical dimension $x$.

Data on the local unit conductance may be applied to the design of an exhaust-gas and air heat exchanger. For example, the life of an exhaust-gas and air heat exchanger may depend on the distribution of temperature within the unit, which depends on the variation of the local unit conductance within the exchanger. Points of high temperature may often cause metal failure, and regions of large temperature gradients cause dangerous thermal stress which decreases the life of the heater. A thorough knowledge of the distribution of the local or point unit thermal conductance $f_{c_x}$ would allow a prediction of these effects, and thus a proper design could be established.

The results of experiments reported herein show that the $f_{c_x}$ in the "entrance section"[1] of a heated circular tube is very much greater than that which would be predicted from equations derived from experiments on very long tubes and depends on the type of fluid entrance. The unit thermal conductance may not reach a constant value as far as 15 tube diameters downstream.[2] The following entrance conditions (fig. 1) were investigated:

(a) Bellmouth
(b) Bellmouth with one screen[3]
(c) Bellmouth with screen holder
(d) Bellmouth with six screens
(e) Right-angle-edge entrance
(f) Bare sharp-edge entrance
(g) Large-orifice entrance
(h) Small-orifice entrance
(i) Short calming section
(j) Long calming section
(k) 45°-angle-bend entrance
(l) 90°-angle-bend entrance
(m) 90°-angle-bend entrance with calming section
(n) 45° round-bend entrance
(o) 90° round-bend entrance
(p) 180° round-bend entrance

---

[1] In this paper the "entrance section" is the initial portion of the tube in which the local unit thermal conductance $f_{c_x}$ is approaching the constant value attained downstream in the tube.

[2] For smooth pipe and constant tube surface temperature.

[3] Iversen (reference 1) obtained experimental data for this case and compared the results with the analyses of Latzko and of Boelter, Martinelli, and associates.

The results of tests (a) to (d) illustrate the effects of turbulence and tests (a), (i), and (j) show the effects of entrance velocity distribution. The remainder of the tests show the effects of the various more practical entrance conditions, in which eddying flow[4] is present.

Latzko (reference 2) developed analytical methods for approximating the variation of the point unit thermal conductance for three entering-gas conditions:

Case I: Both velocity and temperature distributions are uniform over the cross section at the entrance. (This is approximately the actual system of a heating section with a bellmouth at the entrance.)

Case II: The velocity distribution at the entrance corresponds to that for fully developed turbulent flow, and the temperature distribution is uniform over the cross section at the entrance. (The actual system may be visualized as a heating section with a long calming section upstream.)

Case III: The intermediate case between cases I and II, in which the calming section of case II is too short for the fluid to have attained a fully developed velocity distribution before entering the heating section. (See appendix A for description of analytical methods.)

A method noted in reference 3 approximates the variation of the point unit thermal conductance for air for case I. An expression for estimating the integrated average unit thermal conductance for any length of heating sections is also developed in reference 3.

In addition to the point unit thermal conductances, the average unit thermal conductances for the circular tube were calculated as a function of tube length for eight experimental conditions (fig. 1, cases a, b, g, h, i, j, k, and l). For two of these conditions the average unit thermal conductances were analytically obtained by using the equations for $f_{c_x}$

given by Latzko, by Boelter and his associates, and by Iversen.

The average unit thermal conductance, the mean value taken over the entire length of tube in question, is obtained from the following equation

$$f_{c_{av}} = \frac{1}{l} \int_0^l f_{c_x} \, dx$$

The effect of the entering-fluid condition on variations of the average unit thermal conductance with length is presented in table I.

---

[4] A distinction is made in this report between turbulence and eddying flow conditions. Turbulence will be thought of as minute fluctuations of particle velocities; whereas eddying flow is considered to be that characterized by relatively large scale vortices, etc.

<div align="center">DESCRIPTION OF APPARATUS</div>

The apparatus is essentially a doubly steam-jacketed tube through which air flows and is heated. The saturated steam in the inner jacket surrounding the test pipe is condensed by losing heat to the air and is collected at 19 sections along the tube. Heat loss from this inner jacket to the surrounding atmosphere is prevented by the outer jacket containing steam at the same temperature. The rate of condensation of the steam obtained in each section is a measure of the heat-transfer rate occurring in that section. By also measuring the tube wall temperature, the inlet temperature of the air, and the weight rate of air flow, the unit thermal conductance for several entrance conditions (fig. 1) and its variation with length is obtained.

The assembly of the test stand is shown in figure 2. Figure 3 is a drawing of the doubly steam-jacketed tube or the heat exchanger and figures 1 and 4 show the approach sections used and the construction of the bellmouth entrance nozzle. Photographs of the various approach sections are shown in figure 5. Figures 6, 7, 8, and 9 are different views of the apparatus, equipped with a few typical approach sections.

The test pipe is a highly polished seamless steel tube 32 inches long having a 2-inch outside diameter (1.785 in. I.D.). Partitions were brazed to the tube at approximately 1-inch intervals from the leading edge for a distance of 8 inches and then at 2-inch intervals for the remaining length of the tube, to yield 19 separate heating sections. These heating sections contain steam which is condensing because of the heat transferred through the wall of the tube to the cool air.

While traversing through the partitions inside the inner jacket, the uncondensed steam can also enter the glass condensate collector tubes. It will be noticed that the heat of condensation of the steam in the inner

jackets is not only transferred through the test-pipe surface to the air stream but also through the glass condensate collector tubes to the surroundings. The consequent heat loss through the condensate collector glass tubes is a linear function of the height of the condensates in the glass tube because the heat loss is a direct function of the heat-transfer area in the glass tube, which, in turn, varies directly as the height of the condensate. This heat loss occurs even though no heat is transferred through the test section into the air stream; thus it is called the "no-load" heat loss and was used as a correction to the "load" values. The no-load value was about 10 percent of the load values.

The 19 glass condensate collector tubes were installed between a double-glass-partition chamber. This acted as an insulating jacket to reduce the no-load heat losses. Outside of the glass panels a sheet of paper ruled to tenths of an inch was placed in order to measure the water level in the tubes.

The downstream end of the test pipe was connected with a 12-inch-long rubber tube by way of a gate valve to a 3-inch pipe leading to a calibrated orifice section and thence to the intake of a contrifugal blower which exhausted the air to the atmosphere. The rate of air flow was regulated by the blower speed and by means of the gate valve.

Entering-air temperatures were obtained by means of two laboratory thermometers and a thermocouple, all suspended in the air near the entrance. The surface temperatures of the test section were obtained by means of thermocouples imbedded in slots made in the pipe. The downstream outlet-air temperature was obtained by means of a thermocouple in the 3-inch pipe and was arranged for traversing the cross section of the stream.

The equipment was operated with the various entrance apparatus attached to the upstream end of the test section; for instance, a bellmouth nozzle was used to obtain a condition of uniform velocity distribution and wire screens were used to obtain greater turbulence in the air stream. Schematic diagrams of all the entrance effects are shown in figure 1. As shown in figure 5, the short and long calming sections, as well as the two elbows, are made of pipes having the same inside diameter (1.785 in.) as the test pipe. The short calming section is 5 inches long ($l/D_H$ = 2.8) and the long calming section is 20 inches long ($l/D_H$ = 11.2). The legs of both the 45° and 90° elbows are about 2 inches long measured along the central axis. The diameters of the two orifices are 1.04 and 1.41 inches, respectively. The round bends have slightly smaller inside diameters than the test pipe, but the downstream ends are chamfered to give a smooth fit with the test pipe.

## DESCRIPTION OF TESTING PROCEDURE

When steam at atmospheric pressure was admitted to the apparatus at a low flow rate (so adjusted that a strong wisp of steam continuously discharged from the last test section to the atmosphere), the sections were purged of air by the passage of the steam through them and by the steam flow through the glass tube when the corks at the bottoms were removed. As soon as equilibrium temperatures were established throughout, all temperatures and all no-load condensate levels in the glass tubes were recorded at 10-minute intervals for a period of more than 4 hours. Both ends of the test pipe were blocked during this operation. This procedure gave the no-load losses of the system. A duplicate no-load run was also made with the bellmouth nozzle attached and its vacuum pump in operation in order to determine the effect of these attachments.

The test section was then connected to the blower and a constant rate was established. A test procedure, similar to that for the no-load runs, was performed for several air rates with the various entrance conditions shown in figures 1 and 5. Additional data collected were the entrance and exit air temperatures and the weight rate of heated air. All data for load runs were collected at 5-minute intervals. For the entrance conditions employing the bellmouth nozzle, the vacuum pump was adjusted to draw off air at the leading edge of the test section in an attempt to destroy any boundary layer built up along the nozzle surface and thereby to establish a uniform average turbulent velocity distribution at the entrance section of the test pipe.

Possible errors of measurement are the reading of the condensate level, the determination of the no-load condensate rate, and the wall and fluid temperature measurements. The maximum total experimental error is estimated at about 5 percent. The reproducibility of values of $f_{c_x}$ was found to be within 3 percent.

The irregular appearances (as shown in figs. 10 to 20) of erratic values of $f_{c_x}$ at $x/D_H$ of 1.03, 4.41, and 5.25 are attributed to leakage in the condensate tubes; whereas the $f_{c_x}$ at $x/D_H$ of 15.40 and 16.50 are disregarded because of the influence, on the flow condition, of the rubber hose connecter protruding into the back end of the test pipe. Aside from these points, the experimental data indicate a regular variation of $f_{c_x}$ along the pipe length for the different entrance conditions.

## CALCULATIONS

From the data collected, the following items were calculated: the heat gained by the air stream at each section, the temperature rise of the air stream, and finally the local unit thermal conductance at each section.

For some of the entrance conditions (a, b, g, h, i, j, k, and l in fig. 1), the average unit thermal conductance as a function of pipe length was also calculated.

The heat gained by the air stream at each section is equal to the product of the heat of vaporization of water and the difference between the load rate of condensation and the no-load rate of condensation. The no-load rate of condensation varied with the height of the condensate level in the glass tubes. It was a linear variation, however, and so the arithmetic average no-load values between the initial level and the final level of the condensates were used. Thus the heat transfer to the air stream from each section was

$$q_s = \Delta h_{vap} \left( R_{av} - R'_{av} \right)$$

where $R_{av}$ is the average rate of condensation in the glass tube under load, $R'_{av}$ is the average rate of condensation for no load with equal levels of condensate in the glass tube, and $\Delta h_{vap}$ is the heat of vaporization for water at atmospheric pressure.

The temperature rise of the air for each section is obtained by making a heat balance with air. The rate of heat loss by condensation calculated in the preceding paragraph must be equal to the heat gained by the air stream, or

$$q = W c_p \, \Delta t_a$$

where $q$ is the heat loss by the steam for a certain length of the test pipe and $\Delta t_a$, the rise in temperature in this length. (For definition of symbols, see appendix B.) Since the entering-air temperature is measured, the mixed-mean temperature of the air stream at sections of the test pipe must be

$$t_{a_s} = t_{a_0} + \Delta t_a$$

$$= t_{a_0} + \frac{\displaystyle\sum_1^{s-1} q + \frac{q_s}{2}}{W c_p}$$

The local unit thermal conductance for each section is then calculated from the equation

$$q_s = f_{c_x} A \left( t_{a_s} - t_w \right)$$

or

$$f_{c_x} = \frac{q_s}{A\left(t_{a_s} - t_w\right)}$$

where $t_w$, the wall temperature, is obtained experimentally. This is the defining expression for the local unit thermal conductance which, when obtained experimentally, is actually the mean value over the individual heating section.

## DISCUSSION

The variation of the point unit thermal conductance $f_{c_x}$ in the entrance section for 16 entering-air conditions, with Reynolds number Re as a parameter, are shown graphically in figures 10 to 25. In figures 26 to 29, the experimental values of the point unit thermal conductance are compared with those predicted by analytical methods for a particular value of Re. The average unit thermal conductances $f_{c_{av}}$ were calculated and plotted in figures 30 to 37 as a function of the length of pipe.

In recapitulating the equations of heat transfer between a solid surface and air, the following equations are obtained: (See appendix B.)

$$q = f_c A\left(t_w - t_a\right)$$

$$q = -k_a A\left(\frac{\partial t_a}{\partial y}\right)_{y=0}$$

The first equation is the more familiar expression which defines $f_c$, the unit thermal conductance. A consideration of the fluid layer immediately adjacent to the solid surface, into which heat is transferred by pure conduction, yields the second expression (reference 4). Combining the two equations yields,

$$f_c = \frac{-k_a\left(\frac{\partial t_a}{\partial y}\right)_{y=0}}{t_w - t_a}$$

or

$$Nu = \frac{f_c D_H}{k_a} = \frac{-D_H \left(\frac{\partial t_a}{\partial y}\right)_{y=0}}{t_w - t_a}$$

These equations indicate that the point unit thermal conductance is directly proportional to the temperature gradient existing in the fluid next to the wall. In the downstream region beyond the entrance section, by Reynolds' analogy, the temperature gradient is proportional to the velocity gradient for the case where Pr is unity, and a definite relation exists between the velocity gradient and the temperature gradient for other values of Pr (reference 4). In the entrance section, however, even for Pr equal to unity, the relation between velocity and temperature gradients depends upon the type of entrance condition, but it may be stated that, everything else being constant, an increase in the velocity gradient will increase the temperature gradient and thus also the local unit thermal conductance. In the system for which the fluid enters the heating section with a fully developed turbulent velocity distribution, the velocity gradient remains practically unaltered, but the temperature gradient varies from an infinite value at the entrance to the heating section to a finite, constant value far from the entrance section. In contrast, when the temperature and velocity distributions are uniform at the entrance to the tube, both the velocity and temperature gradients vary from an infinite value at the tube entrance to a finite, constant value far from the entrance section.

As mentioned in the foregoing paragraph, for turbulent flow through pipes with the velocity and temperature distributions uniform over the cross section at entrance, both the velocity and temperature gradients at the surface will decrease from an infinite value at the entrance to some finite value downstream. The growth of the so-called turbulent boundary layer (reference 5) accompanies these changes. Unless a turbulence promoter is used, a laminar boundary layer will usually precede the turbulent boundary layer, as shown in the following diagrams.

Growth of
boundary
layers

Variation of
velocity
distribution

$f_{c_x}$

Laminar
boundary
layer

Turbulent boundary
layer

Fully established
velocity distribution

$x/D_H$
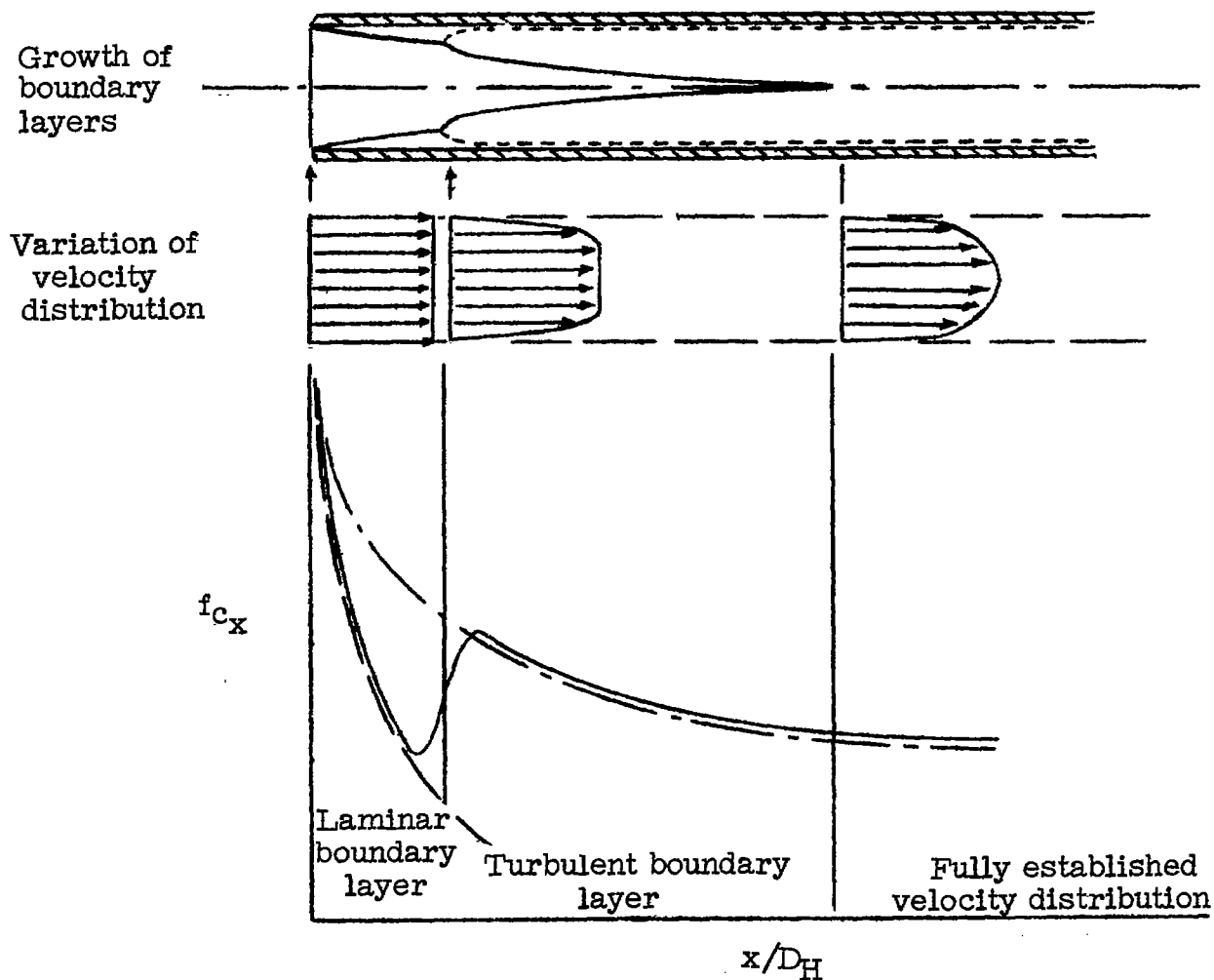
In these diagrams are shown the typical growths of the laminar and
turbulent boundary layers, the variation of the velocity distribution
along the length of the pipe, and a plot of the point unit thermal con-
ductance against the distance along the tube. The dashed line in the plot
of $f_{c_x}$ against $x/D_H$ is the variation of $f_{c_x}$ for laminar flow, and

the dot—dash line is the variation of $f_{c_x}$ for turbulent flow. The solid line would be a predicted variation of the point unit thermal conductance. The local unit thermal conductance $f_{c_x}$ would rapidly decrease from an infinite value in the laminar flow region and increase at the point where the flow changes from laminar to turbulent (location usually unknown) and then decrease again, as may be predicted from the variation (along the tube) of the temperature gradient at the wall. From the point where the temperature distribution is fully developed (the temperature gradient would then be constant), $f_{c_x}$ should be constant with distance along the tube.

The curves showing the variation of $f_{c_x}$ in figure 10 (bellmouth—entrance condition) exhibit this expected dip at the low Reynolds numbers. Figure 11 (bellmouth with one screen) shows that the addition of a screen as a turbulence promoter eliminates the dips which are due to the presence of the laminar boundary layer. The addition of more screens as shown in figure 13 to increase turbulence (not eddying flow) does not increase $f_{c_x}$ appreciably.

The entrance condition with a fully developed turbulent velocity distribution but a uniform temperature at the entrance will illustrate the rapidity with which the temperature distribution becomes fully developed. These experimental values of $f_{c_x}$ are shown in figure 19 (long—calming—section entrance condition). Figure 18 (short—calming—section entrance) is an approximate illustration of case III (mentioned in INTRODUCTION), for which Latzko proposed a graphical solution.

For the case in which the air enters through a bare sharp—edge entrance a stagnant air pocket may develop at the leading edge, yielding an appreciable resistance to heat transfer. The curves in figure 15 (bare, sharp—edge entrance condition) confirm this phenomenon. The
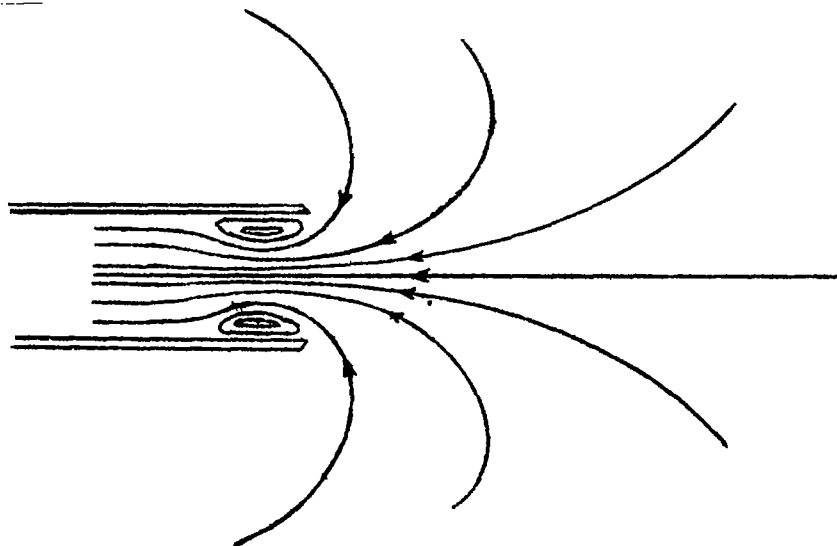
introduction of the large baffle in condition  e, figure 1 (right-angle-edge entrance) reduces the size of the air pocket and also the resistance to heat transfer as shown by the results of figure 14. The presence of orifices at the entrance enlarges the air pocket and shifts the point of high heat transfer farther downstream. (See figs. 16 and 17 for experimental verification.)

The flow conditions affected by the presence of angle bends and round bends at the entrance are complex but approach conditions for many practical installations. The degree of turbulence is probably increased. Eddying flow is present, and a stagnant air pocket may also exist. The velocity distribution is no longer symmetrical about the axis of the pipe (see reproduced photographs showing flow around bends, fig. 38). Experimental data are given in figures 20 to 25 for the following conditions; 45° angle bend, 90° angle bend, 90° angle bend with a long calming section, 45° round bend, 90° round bend, and 180° round bend. Notice that the results using the 90° angle bend were not seriously affected by the addition of the long calming section.

The point-unit thermal conductance  $f_{c_x}$  as predicted by the various analytical methods presented in the appendix are plotted in figure 26 at a particular value of Re (~50,000) for comparison. It may be seen that values of  $f_{c_x}$  given by the equations of Latzko (equations (A1) and (A2)) and Iversen's simplifications (equations (A5) and (A6)) are about 20 percent lower than those given by the expressions of Boelter, Martinelli, and associates (equations (A9) and (A10)). It should be

noted here that the value of $f_{c_{av}}$ predicted by means of equations (A9)
and (A10) are about 3 percent lower than the accepted expression in
reference 6, which was obtained by analyzing large quantities of data
taken for long pipes. The fourth curve in this graph (fig. 26) is a
plot of Latzko's equation (A13) for case II, in which the initial
velocity distribution is that of fully developed turbulent flow and the
initial temperature distribution is uniform.

The equations of Latzko and of Boelter, Martinelli, and associates,
previously mentioned, are compared with experimental values in figure 27.
The four experimental $f_{c_x}$ curves are obtained, for one Re ($\sim$50,000),
from figures 10 to 13 which include the following entrance conditions:
bellmouth only, bellmouth with one screen, bellmouth with screen holder,
and bellmouth with six screens. It will be noticed that the experimental
curves lie between the two analytical curves and that the increase in the
degree of turbulence by means of screens affects the values of $f_{c_x}$ only
slightly. Both methods of predicting the point unit thermal conductances
are within 10 percent of the experimental values.

Figure 28 indicates that Latzko's equation (A13) is not reliable in
the prediction of $f_{c_x}$ for case II (initial temperature distribution is
uniform and initial velocity distribution is that of fully developed
turbulent flow). Values predicted by the equation are from 10 to
30 percent low. Note also that the experimental results of $f_{c_x}$ for
short—calming—section entrance, right—angle—edge entrance, and bare sharp—
edge entrance are all higher than equations (A9) and (A10), for values
of $x/D_H$ less than about 10.

The comparison in figure 29 of the various bends used at the entrance
yields some interesting results which are tentatively explained as follows:
For sharp—angle bends the change from 45° to 90° increases the $f_{c_x}$,
whereas for smooth bends the reverse is true. This effect indicates that
apparently for sharp—angle bends the effect of eddying flow predominates,
so that the increased eddying flow produced by the 90° bend increases the
rate of heat transfer at the tube entrance. For round bends, however,
since eddying is not so pronounced, the 45° bend yields higher heat—transfer
rates by acting as a short calming section. In the case of the 180° round
bends, the high $f_{c_x}$ may be explained by the fact that the centrifugal
force developed in the bend increased the velocity gradient at the bottom
region of the circular pipe and thus produced the higher heat—transfer
rate. All these explanations are tentative, of course, and must be checked
by further experiments designed to prove or disprove these arguments.

In figure 30, the following entrance conditions are compared
(at  Re ∼ 27,000):  right—angle—edge entrance, bare sharp—edge entrance,
large—orifice entrance, small—orifice entrance, and 90°—angle—bend
entrance.  The extremely high values of point unit thermal conductances
resulting from the orifice—entrance condition should be noted.  The shift
of the point of maximum heat transfer is accompanied by the shift of the
point of high temperature gradient in the wall.  The location of this
point of high temperature gradient is important in certain thermal—
stress problems.

Figures 28, 29, and 30 show that none of the equations derived
analytically for predicting  $f_{c_x}$  could be used for the following

entrance conditions:  right—angle—edge entrance, bare sharp—edge entrance,
orifice entrance, short—calming—section entrance, 45°—angle—bend and
round—bend entrance, 90°—angle—bend and round—bend entrance, and the
180°—round—bend entrance.

In figures 31 to 37 and 39 are shown calculated values of the
average unit thermal conductance  $f_{c_{av}}$  as a function of  $l/D_H$  with the

parameter  Re.  If the ratio  $f_{c_{av}}/f_{c_\infty}$  is plotted against  $D_H/l$  on

Cartesian coordinates, an approximate linear relation is obtained for
values of  $l/D_H$  greater than 5.  An equation of the following form
is useful to represent the average value of  $f_c$  for the length  $l$.
(See appendix A.)

$$f_{c_{av}} = f_{c_\infty}\left(1 + K\frac{D_H}{l}\right)$$

The values of  K  as a function of  Re  and  Pr,  as derived from
analytical methods and the graphs of  $f_{c_{av}}/f_{c_\infty}$  against  $D_H/l$,  are listed

in table I.

## CONCLUSIONS

From an investigation of the distribution of heat—transfer rate that
results from a variation of the unit thermal conductance at the entrance
to a tube for various entering—fluid conditions the following conclusions
were made:

1.  The magnitudes as well as the variation of the point—unit thermal
conductance  $f_{c_x}$   in the entrance section of a tube, and consequently the

magnitudes and the variation of the average unit thermal conductance $f_{c_{av}}$, depend greatly on the entering-fluid conditions.

2. The values of $f_{c_\infty}$, the unit thermal conductance downstream

when both the velocity and temperature distributions are fully developed, are practically independent of the entering-fluid conditions.

3. The effect on the unit thermal conductance of increasing the degree of turbulence by addition of screens is negligible.

4. Only one ideal system of turbulent flow in circular tubes has been successfully analyzed. For case I, in which the velocity and temperature distributions are uniform at the entrance, the point unit thermal conductances were predicted by two methods to within 10 percent of the experimental data.

5. Values of the average unit thermal conductance for $l/D_H$ greater than about five may be approximated by the equation $f_{c_{av}} = f_{c_\infty}\left(1 + K\dfrac{D_H}{l}\right)$.

The coefficient $K$ is given for eight entrance conditions in table I.

Department of Engineering
       University of California
              Berkeley, Calif., Jan. 3, 1945

## APPENDIX A

## ANALYTICAL METHODS

Existing analytical methods for predicting the variation of the point unit thermal conductance along the entrance section are confined to certain ideal cases only. The systems analytically investigated are:

Case I: The velocity and temperature distributions at entrance are uniform over the cross section (similar to condition b, fig. 1).

Case II: The temperature distribution is uniform over the cross section at the entrance but the velocity distribution is that of the established turbulent flow distribution (similar to condition j, fig. 1).

Case III: The intermediate between cases I and II, in which the calming section of case (II) is too short for the fluid to have attained complete hydrodynamic flow before entering the heating section (approximately similar to condition i, fig. 1).

### Case I

Latzko (reference 2) gave for case I the following equations for the point unit thermal conductance:

(a)   for $\dfrac{x}{D_H} < \left( \dfrac{l_0}{D_H} = 0.625 \ Re^{0.25} \right)$

where $l_0$ is the length of the entrance section, that is, the distance to the point where the temperature distribution has attained its fully developed form.

$$f_{c_x} = 0.0384 \ \frac{Gc_p}{Re^{0.25}} \ B' = f_{c_\infty} B' \qquad\qquad (A1)$$

where

$$B' = \frac{1.143 - 0.032\xi + 0.00148\xi^{1.865}}{1.340\left(4\xi^2 - 22\xi + 165\right)^{3/4}\xi^{1/4}\left[1 - 0.133\xi + 0.024\xi^2 + \left(0.00148\xi^{1.865} - 0.032\xi\right)\left(0.52\xi - 0.14\xi^2\right)\right]}$$

and $\xi = \dfrac{\delta}{r} = 1.41\ Re^{-1/5}\left(\dfrac{x}{D_H}\right)^{4/5} - 0.048\ Re^{-2/5}\left(\dfrac{x}{D_H}\right)^{8/5} + 0.168\ Re^{-3/5}\left(\dfrac{x}{D_H}\right)^{12/5}$

(b) for $\dfrac{x}{D_H} > \left(\dfrac{l_0}{D_H} = 0.625\ Re^{0.25}\right)$

$$f_{c_x} = 0.0384\frac{Gc_p}{Re^{0.25}}\left(\frac{0.874e^{\frac{-0.1510}{Re^{0.25}}\frac{x}{D_H}} + 0.0298e^{\frac{-2.844}{Re^{0.25}}\frac{x}{D_H}}}{0.873e^{\frac{-0.1510}{Re^{0.25}}\frac{x}{D_H}} + 0.0068e^{\frac{-2.844}{Re^{0.25}}\frac{x}{D_H}}}\right) \tag{A2}$$

$$= f_{c_\infty}B''$$

where $B''$ is the term in parentheses in equation (A2).

By graphically obtaining $B'_{av}\left(= \dfrac{1}{\psi}\displaystyle\int_0^{\psi} B'\ d\psi\right)$ as a function of $\psi = Re^{-1/5}\left(\dfrac{l}{D_H}\right)^{4/5}$ the average unit thermal conductance $f_{c_{av}}$ could be obtained in terms of $l$, the tube length measured from the leading edge.

(a)   For   $\psi < 0.686$   or   $\dfrac{l}{D_H} < \left( \dfrac{l_0}{D_H} = 0.625\ Re^{0.25} \right)$

$$f_{c_{av}} = B'_{av}\ f_{c_\infty} = 1.11 \psi^{-0.275} f_{c_\infty} = 1.11\ f_{c_\infty} \left[ Re^{-1/5} \left( \dfrac{l}{D_H} \right)^{4/5} \right]^{-0.275} \tag{A3}$$

(b)   For   $\psi > 0.686$   or   $\dfrac{l}{D_H} > \left( \dfrac{l_0}{D_H} = 0.625\ Re^{0.25} \right)$

$$f_{c_{av}} = \left[ 1.11\ f_{c_\infty}(0.686)^{-0.275} \dfrac{l_0}{D_H} + f_{c_\infty} \left( \dfrac{l}{D_H} - \dfrac{l_0}{D_H} \right) \right] \dfrac{D_H}{l}$$

$$= f_{c_\infty} \left( 1 + 0.144\ Re^{0.25} \dfrac{D_H}{l} \right) \tag{A4}$$

Iversen (reference 1) was successful in simplifying the complex equations given by Latzko, and presented the following equations for the variation of the point unit thermal conductance in the entrance section with initially uniform velocity and temperature distributions.

(a)   For   $\dfrac{x}{D_H} < Re^{1/4}$

$$f_{c_x} = 0.0384\ Gc_p \dfrac{1}{Re^{0.2214}} \left( \dfrac{D_H}{x} \right)^{0.1144} \tag{A5}$$

(b)   For   $\dfrac{x}{D_H} > Re^{1/4}$

$$f_{c_\infty} = 0.0384\ Gc_p \left( \dfrac{1}{Re} \right)^{1/4} \tag{A6}$$

For the average unit thermal conductance for a length $l$, he gave:

(a)  For  $\dfrac{l}{D_H} < Re^{1/4}$

$$f_{c_{av}} = 0.0434 \, Gc_p \, \frac{1}{Re^{0.2214}} \left(\frac{D_H}{l}\right)^{0.1144} \tag{A7}$$

(b)  For  $\dfrac{l}{D_H} > Re^{1/4}$

$$f_{c_{av}} = f_{c_\infty}\left(1 + 0.128 \, Re^{0.25} \, \frac{D_H}{l}\right) \tag{A8}$$

The method of Martinelli (reference 3) presents an approximate method of solving case I by postulating that the fluid flow along the entrance section is similar to that along a flat plate until the boundary layer builds up to the radius of the pipe. Thus he gives for air flowing turbulently in the entrance section the following equations[1] for the point unit thermal conductance.

(a)  For  $\dfrac{x}{D_H} < 4.4$

$$f_{c_x} = 7.3(10)^{-4} \, \frac{T_f^{0.3} G^{0.8}}{x^{0.2}} \tag{A9}$$

(b)  For  $\dfrac{x}{D_H} > 4.4$

$$f_{c_x} = 5.4(10)^{-4} \, T^{0.3} \, \frac{G^{0.8}}{D_H^{0.2}} \tag{A10}$$

---

[1]Beginning with part XVIII of this series, the exponent of $T$ (and $T_f$) and the constants in these equations have been simplified.

And for the average unit thermal conductance as a function of length,

(a)  For $\dfrac{l}{D_H} < 4.4$

$$f_{c_{av}} = 9.1(10)^{-4} \frac{T_f^{0.3} G^{0.8}}{l^{0.2}} \tag{A11}$$

(b)  For $\dfrac{l}{D_H} > 4.4$

$$f_{c_{av}} = 5.4(10)^{-4} \frac{T^{0.3} G^{0.8}}{D_H^{0.2}} \left(1 + 1.1 \frac{D_H}{l}\right)$$

$$= f_{c_\infty}\left(1 + 1.1 \frac{D_H}{l}\right) \tag{A12}$$

## Case II

For this system, where the temperature distribution is uniform over the cross section at the entrance but the velocity distribution is that for fully developed flow, Latzko presents the following equation for the point unit thermal conductance for values of $x/D_H$ from $0$ to $\infty$.

$$f_{c_x} = 0.0346 \frac{G c_p}{Re^{0.25}} \frac{1.078 e^{\frac{-0.1510}{Re^{0.25}}\frac{x}{D_H}} + 0.134 e^{\frac{-2.844}{Re^{0.25}}\frac{x}{D_H}} + 0.980 e^{\frac{-29.42}{Re^{0.25}}\frac{x}{D_H}}}{0.970 e^{\frac{-0.1510}{Re^{0.25}}\frac{x}{D_H}} + 0.024 e^{\frac{-2.844}{Re^{0.25}}\frac{x}{D_H}} + 0.006 e^{\frac{-29.42}{Re^{0.25}}\frac{x}{D_H}}}$$

$$= \frac{0.0384}{Re^{0.25}} G c_p \left(1 + 0.1 e^{\frac{-2.7}{Re^{0.25}}\frac{x}{D_H}} + 0.9 e^{\frac{-29.27}{Re^{0.25}}\frac{x}{D_H}} - 0.023 e^{\frac{-31.96}{Re^{0.25}}\frac{x}{D_H}}\right)$$

$$= f_{c_\infty} B''' \tag{A13}$$

where $B'''$ is the term in parentheses.

The average unit thermal conductance as a function of tube length is obtained by direct integration.

(a) For all values of $l/D_H$

$$f_{c_{av}} = f_{c_{\infty}} \left[ 1 + 0.067 \, Re^{0.25} \frac{D_H}{l} + \right.$$

$$\left. \frac{D_H}{l} \left( \frac{0.1}{2.7} Re^{0.25} e^{Re^{0.25} \frac{-2.7}{D_H} \frac{l}{D_H}} + \frac{0.9}{29.27} Re^{0.25} e^{Re^{0.25} \frac{-29.27}{0.25} \frac{l}{D_H}} + \frac{0.023}{31.96} Re^{0.25} e^{Re^{0.25} \frac{-31.96}{0.25} \frac{l}{D_H}} \right) \right] \quad \text{(A14)}$$

(b) For $\frac{l}{D_H} > (\sim 5)$ the following may be used

$$f_{c_{av}} = f_{c_{\infty}} \left( 1 + 0.067 \, Re^{0.25} \frac{D_H}{l} \right) \quad \text{(A15)}$$

## Case III

For case III Latzko offers the following approximate graphical method. First the point unit thermal conductance at the particular Re of the problem is calculated as if it were for case I, and then the calculation is repeated as if it were for case II. Both curves for the point unit thermal conductances are laid out at a distance of $x_0/D_H$ apart, equal to the distance between the beginning of the calming section and the heating section, with the $f_{c_x}$ calculated for case I ahead of that for case II. The "envelope" of the two curves would be the solution for the first approximation.

For example,
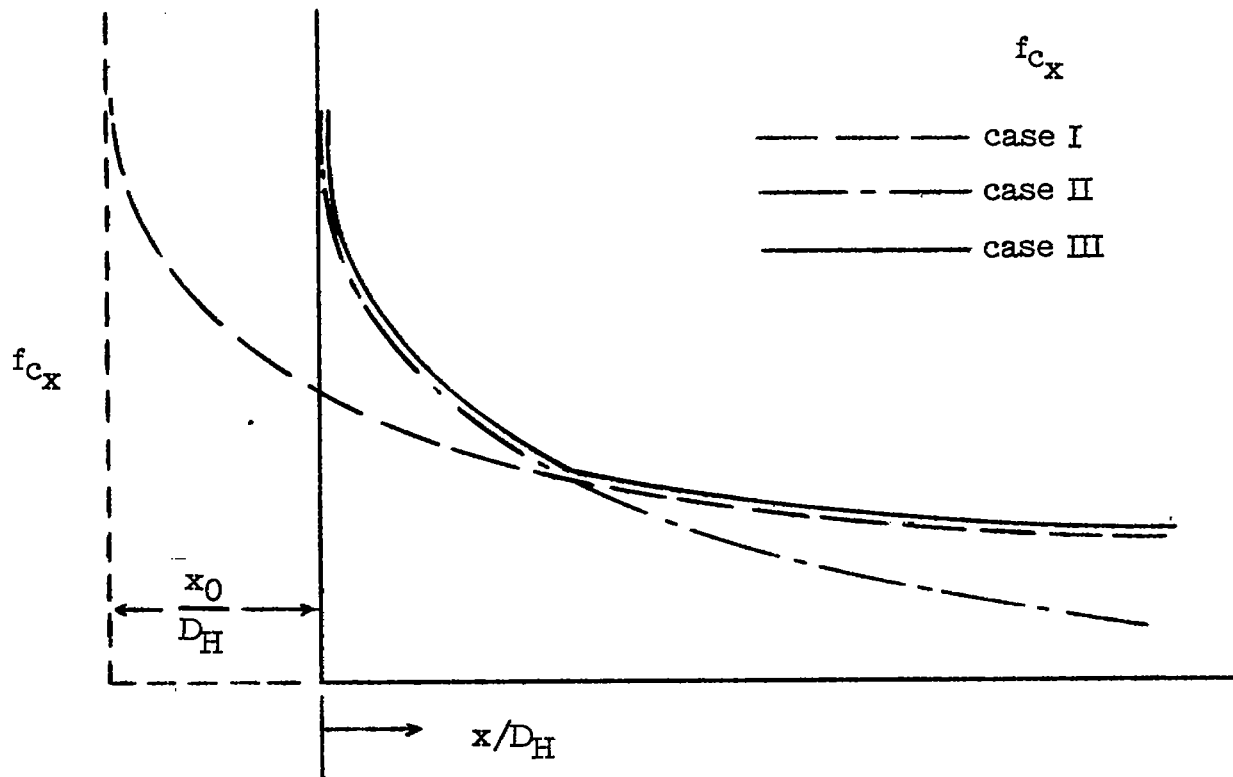
# APPENDIX B

## SYMBOLS

| | |
|---|---|
| $A$ | heat-transfer area perpendicular to heat flow, sq ft |
| $A_c$ | cross-sectional area of tube, sq ft |
| $B'$, $B''$, $B'''$, $B'_{av}$ | functions defined in appendix A |
| $c_p$ | specific heat of fluid at constant pressure, Btu/(lb)(°F) |
| $D_H$ | hydraulic diameter of tube $\left(\dfrac{4 \times \text{Cross-sectional area}}{\text{Wetted perimeter}}\right)$, ft |
| $f_c$ | unit thermal conductance between pipe and fluid, Btu/(hr)(sq ft)(°F) |
| $f_{c_{av}}$ | average unit thermal conductance in length $l$ of tube, Btu/(hr)(sq ft)(°F) |
| $f_{c_x}$ | local or point unit thermal conductance, x feet from entrance of tube, Btu/(hr)(sq ft)(°F) |
| $f_{c_\infty}$ | point unit thermal conductance downstream of the entrance of tube where the temperature distribution in the fluid is fully developed, Btu/(hr)(sq ft)(°F) |
| $G$ | weight flow of air per unit cross-sectional area $\left(\dfrac{W}{A}\right)$, lb/(hr)(sq ft) |
| $\Delta h_{vap}$ | heat of vaporization of water at atmospheric pressure, Btu/lb |
| $k_a$ | thermal conductivity of air, Btu/(hr)(sq ft) (°F/ft) |
| $K$ | coefficient defined by equation $f_{c_{av}} = f_{c_\infty}\left(1 + K \dfrac{D_H}{l}\right)$ |
| $l$ | tube length measured from the leading edge, ft |
| $l_0$ | length of entrance section, ft |
| $q$ | radial rate of heat transfer, Btu/hr |

$q_s$            radial rate of heat transfer per section, Btu/hr

$r$              radius of test pipe, ft

$R_{av}$         rate of condensation for load runs, lb/hr

$R'_{av}$        rate of condensation for no-load runs, lb/hr

$T$              arithmetic average of mixed-mean absolute tempera-
                 ture of air entering and leaving tube, $^\circ R$

$T_f$            arithmetic average of mixed-mean air temperature
                 and tube-wall temperature $\left[\left(\dfrac{t_w + t_a}{2}\right) + 460\right]$, $^\circ R$

$t_w$            tube-wall temperature, $^\circ F$

$t_a$            air temperature, $^\circ F$

$t_{a_0}$        mixed-mean air temperature at entrance, $^\circ F$

$t_{a_s}$        mixed-mean air temperature at any particular
                 section, $^\circ F$

$W$              weight rate of fluid, lb/hr

$x$              distance from entrance of tube, ft

$y$              distance into fluid stream measured from the tube
                 wall, ft

$\gamma$         specific weight of fluid, lb/cu ft

$\delta$         thickness of boundary layer, ft

$\mu$            absolute viscosity of fluid, (lb)(sec)/sq ft

$\nu$            kinematic viscosity of fluid, sq ft/sec

$\xi$            dimensionless ratio of distance $\left(\dfrac{\delta}{r}\right)$

$\rho = \dfrac{\gamma}{g}$   mass density of fluid, $(lb)(sec^2)/ft^4$

$\psi$           function defined in appendix A

$Nu$             Nusselt number $\left(\dfrac{f_c D_H}{k}\right)$

Re            Reynolds number $\left(\dfrac{vD_H}{\nu} = \dfrac{GD_H}{3600\mu g}\right)$

Pr            Prandtl number $\left(\dfrac{3600g\mu c_p}{k}\right)$

REFERENCES

1. Iversen, H. W.: Variation of the Point Unit Thermal Conductance on Entrance to Tubes for a Fluid Flowing Turbulently. M.S. Thesis, Univ. of Calif., 1943.

2. Latzko, H.: Heat Transfer in a Turbulent Liquid or Gas Stream. NACA TM No. 1068, 1944.

3. Boelter, L. M. K., Dennison, H. G., Guibert, A. G., and Morrin, E. H.: An Investigation of Aircraft Heaters. X — Measured and Predicted Performance of a Fluted-Type Exhaust Gas and Air Heat Exchanger. NACA ARR, March 1943.

4. Boelter, L. M. K., Martinelli, R. C., and Jonassen, F.: Remarks on the Analogy between Heat Transfer and Momentum Transfer. Trans. A.S.M.E., vol. 63, July 1941, pp. 447-455.

5. Prandtl, L.: The Mechanics of Viscous Fluids. Vol. III of Aerodynamic Theory, div. G, W. F. Durand, ed., Julius Springer (Berlin), 1935.

5. McAdams, William H.: Heat Transmission. Second ed., McGraw-Hill Book Co., Inc., 1942, pp. 168, 171.

TABLE I

$$\left[ \frac{l}{D_H} > 5 \right]$$

| Entrance conditions | K |
|---|---|
| Bellmouth<br><br>    Experimental | 0.7 |
| Bellmouth with one screen<br><br>    Equation (A4)<br>    Equation (A12)<br>    Equation (A8)<br>    Experimental | $0.144 \text{ Re}^{0.25}$<br>1.1<br>$0.128 \text{ Re}^{0.25}$<br>1.2 |
| Short calming section with sharp-edge entrance<br><br>    Experimental | ~3 |
| Long calming section with sharp-edge entrance<br><br>    Equation (A15)<br>    Experimental | $0.067 \text{ Re}^{0.25}$<br>1.4 |
| $45^\circ$-angle-bend entrance<br><br>    Experimental | ~5 |
| $90^\circ$-angle-bend entrance<br><br>    Experimental | ~7 |
| 1-inch-square-edge-orifice entrance<br><br>    Experimental | ~16 |
| $1\frac{1}{2}$-inch-square-edge-orifice entrance<br><br>    Experimental | ~7 |

NACA

(a) Bellmouth.

(b) Bellmouth with one screen.

(c) Bellmouth with screen holder.

(d) Bellmouth with six screens.

(e) Right-angle-edge entrance.

(f) Bare sharp-edge entrance.

(g) Large-orifice entrance.

(h) Small-orifice entrance.

(i) Short calming section.

(j) Long calming section.

(k) 45°-angle-bend entrance.

(l) 90°-angle-bend entrance.

(m) 90°-angle-bend with calming section.

(n) 45° round-bend entrance.

(o) 90° round-bend entrance.

(p) 180° round-bend entrance.

Figure 1.- Entrance conditions.

1. Two thermometers and thermocouple for inlet temp.
2. Approach section (see fig. 1)
3. Steam throttle valve
4. Test pipe (see fig. 3)
5. Steam jacket
6. Steam relief to atmosphere
7. Rubber connector
8. Gate valve for adjusting air rate
9. Thermocouple for final air temp.
10. Glass tubes (condensate collectors)

11. 20 thermocouples for tube-wall temp.
12. Condensate drain
13. Water manometer for orifice pressure
14. Orifice
15. Draft gage for orifice differential pressure
16. Thermocouple for orifice temp.
17. Blower suction
18. Blower discharge to atmosphere
19. Resistance box
20. 110-volt d.-c. for blower motor

Figure 2.- Test-stand assembly.

Section A-A    Figure 3.- Heat exchanger.

1. 1/4-inch steam inlet
2. Steam jacket
3. 3-inch pipe segments
4. Partition
5. Leading edge
6. Condensate tubes
7. 1/4-inch hole to tubes
8. 1/16-inch rubber gasket
9. 1/8-inch rubber gasket
10. Scale behind all tubes
11. 1/2-inch drain
12. Steam to atmosphere
13. Rubber tube connector
14. 1/4-inch hole for steam passage
15. Slots for thermocouples

Note: (1) 20 thermocouples for tube-wall temperatures soldered to corners of grooves; 5 in each groove spaced evenly. Grooves filled with Smooth-On. (2) Steam at atmospheric pressure throughout. (3) First section 1.31 inches long; sections 2 to 8 approximately 1 inch long; sections 9 to 19 approximately 2 inches long.

Section A-A

1. 1/4-inch mesh wire screen over intake
2. Strings to induce turbulence
3. A.S.M.E. nozzle shape
4. 1/8- by 1/8-inch collector ring
5. 1/16-inch spacer
6. Back plate
7. Test pipe
8. Leading edge of test pipe
9. 1/4-inch tubes to vacuum pump

Note: Strings allowed to wave freely.
Screen over the whole intake area.

Figure 4.- Bellmouth.
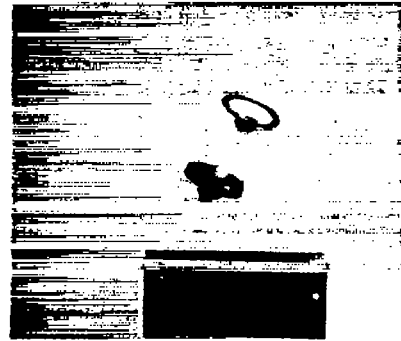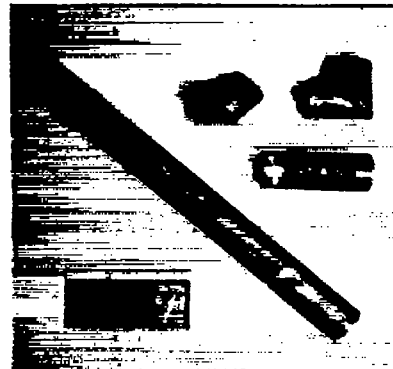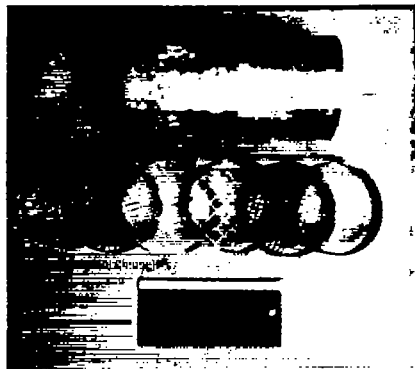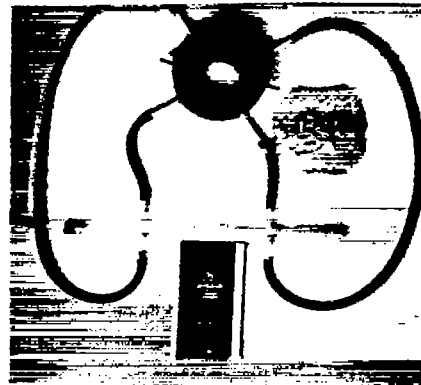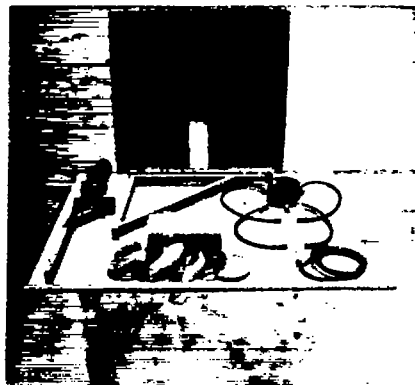
Figure 5.- Photographs of approach sections.
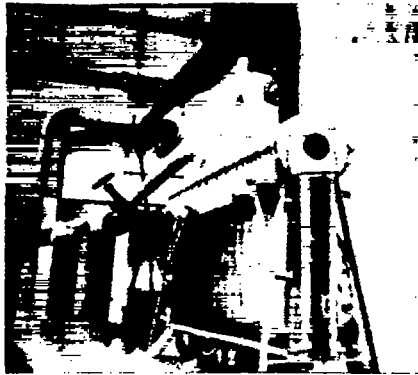
Figure 6.-   Front view and bare sharp-edge entrance condition.
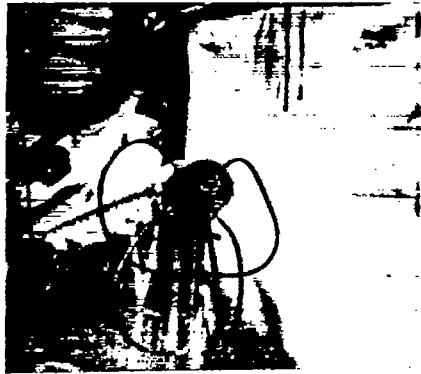


Figure 7.-   Bellmouth entrance.     Figure 8.-   Short calming section.
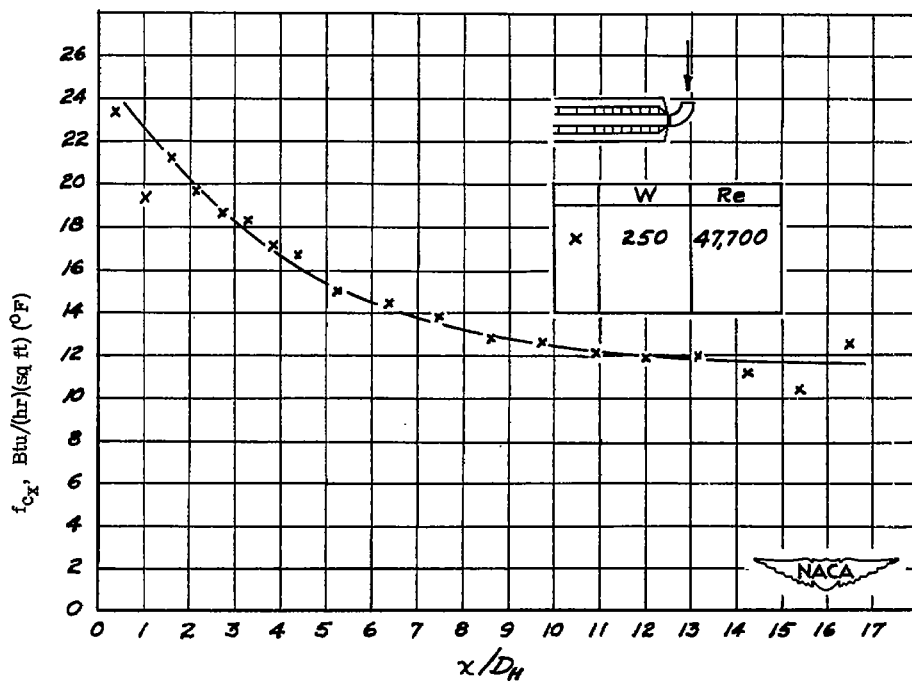


Figure 9.-   45°-angle bend.
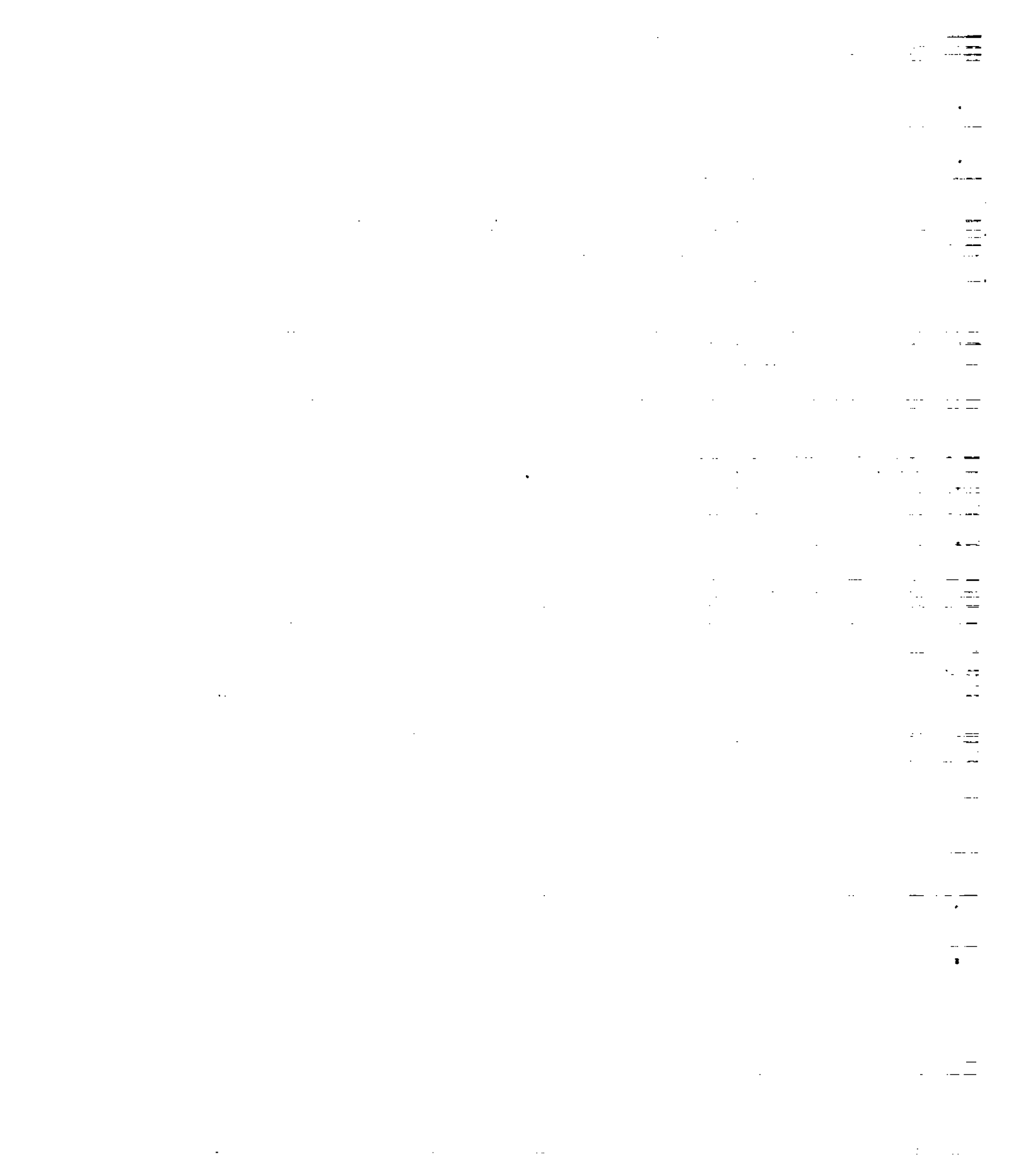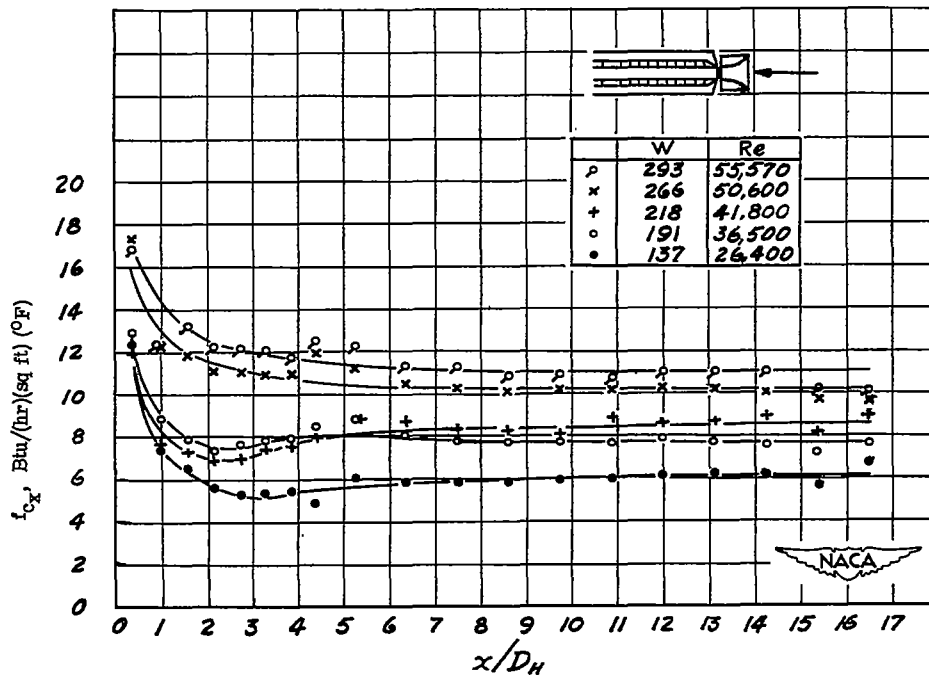
Figure 10.- Variation of point unit thermal conductance in circular tube with bellmouth at entrance.
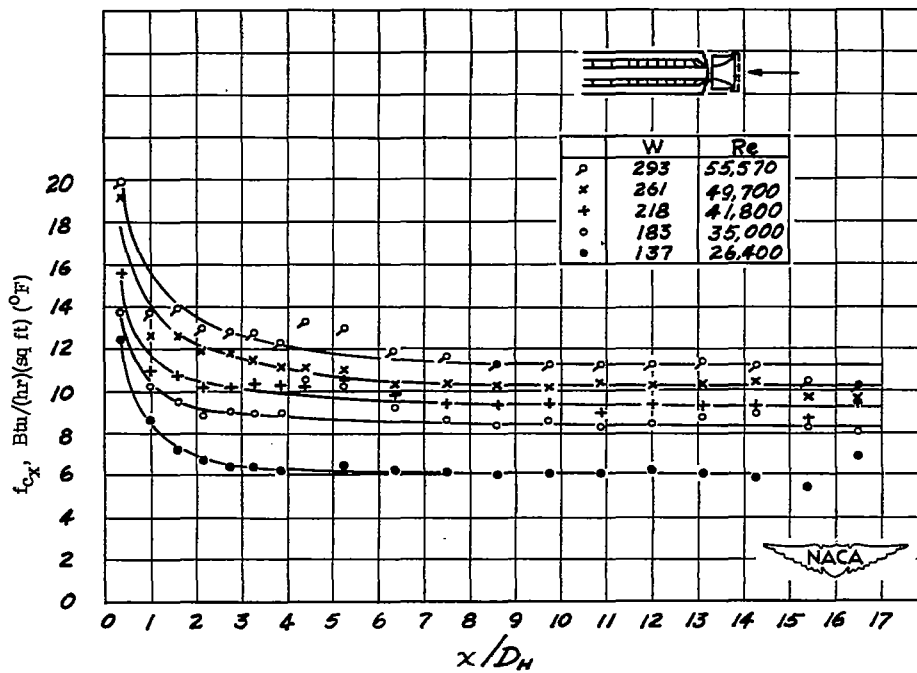


Figure 11.- Variation of point unit thermal conductance in circular tube with bellmouth and one screen at entrance.
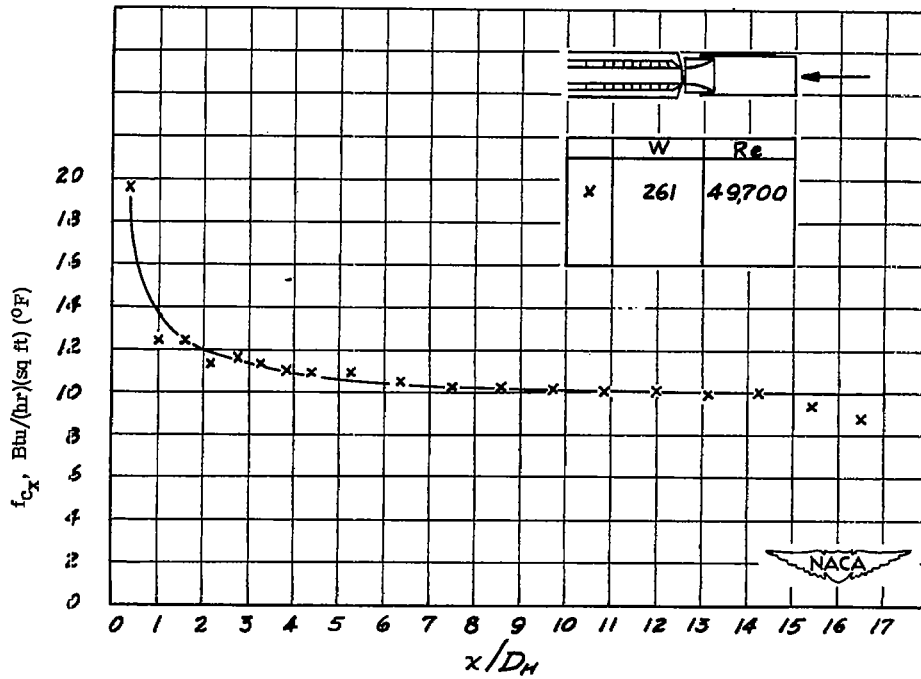
Figure 12.- Variation of point unit thermal conductance in circular tube with bellmouth and screen holder at entrance.
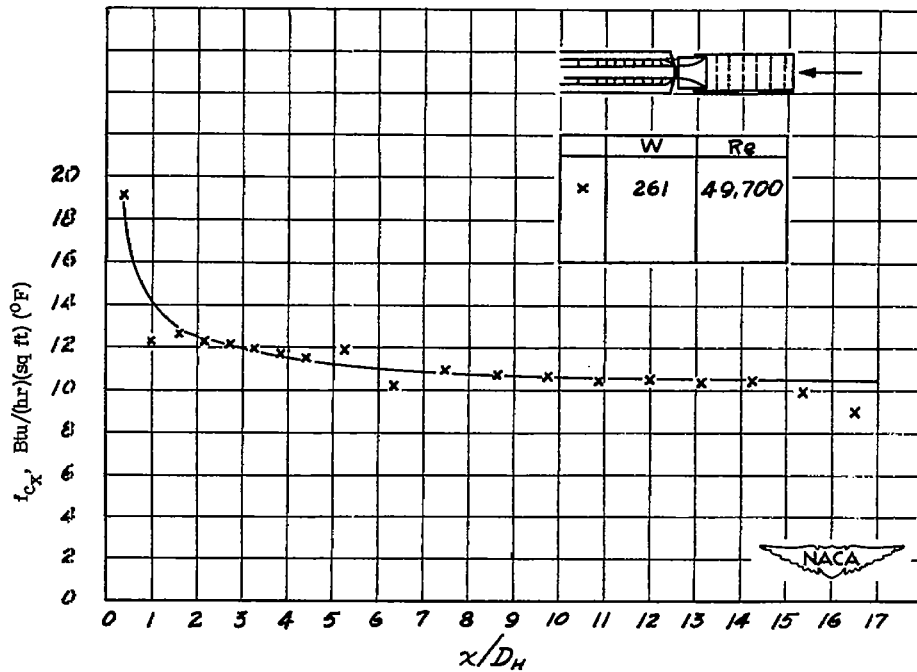


Figure 13.- Variation of point unit thermal conductance in circular tube with bellmouth and six screens at entrance.
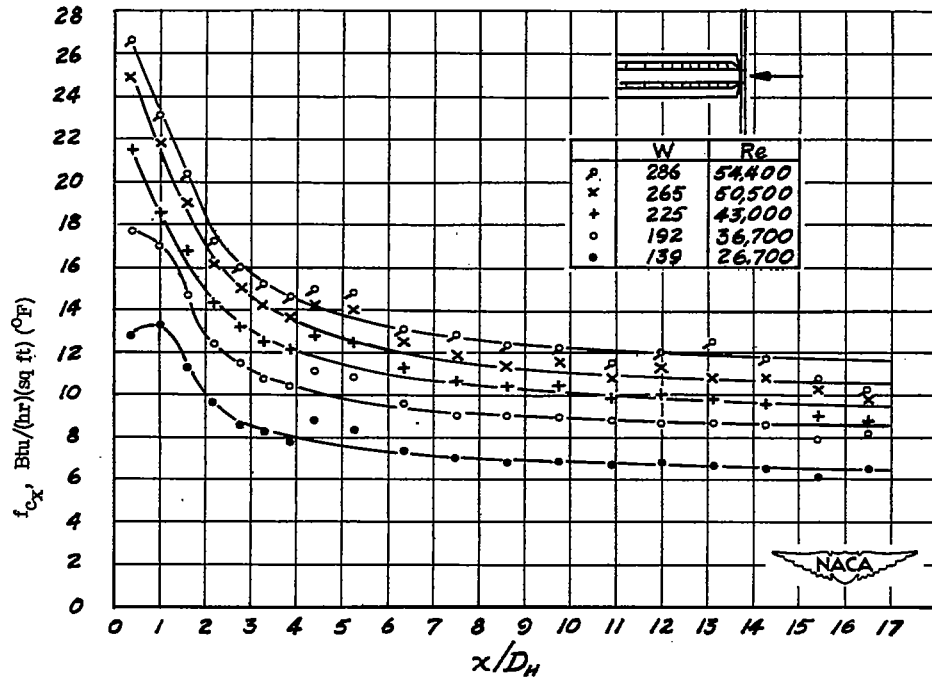
Figure 14.- Variation of point unit thermal conductance in circular tube with right-angle-edge entrance.

| | W | Re |
|---|---|---|
| ρ | 286 | 54,400 |
| x | 265 | 50,500 |
| + | 225 | 43,000 |
| o | 192 | 36,700 |
| • | 139 | 26,700 |
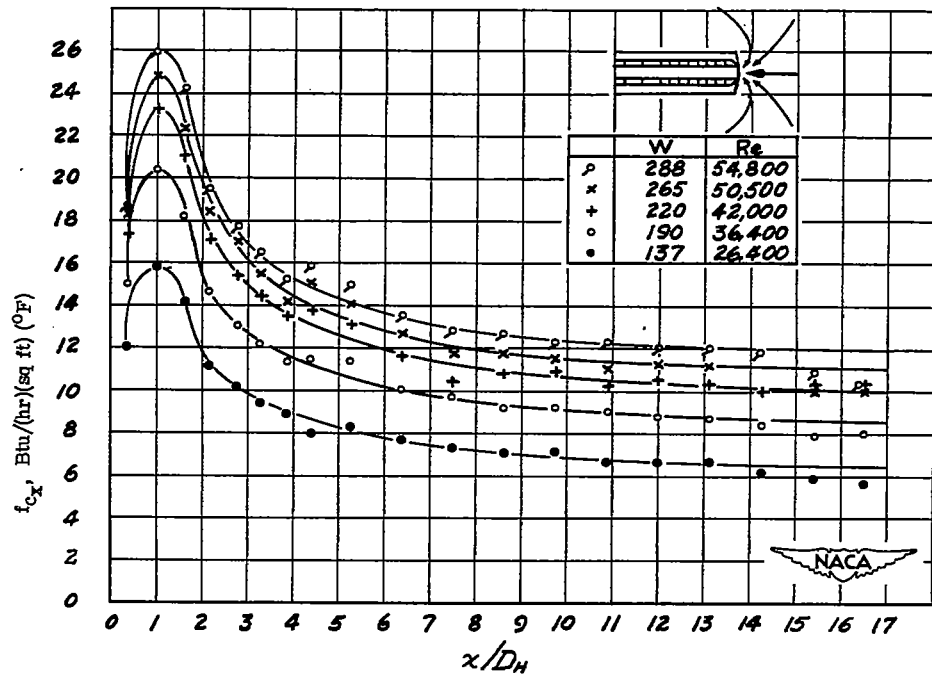


Figure 15.- Variation of point unit thermal conductance in circular tube with bare sharp-edge entrance.

| | W | Re |
|---|---|---|
| ρ | 288 | 54,800 |
| x | 265 | 50,500 |
| + | 220 | 42,000 |
| o | 190 | 36,400 |
| • | 137 | 26,400 |
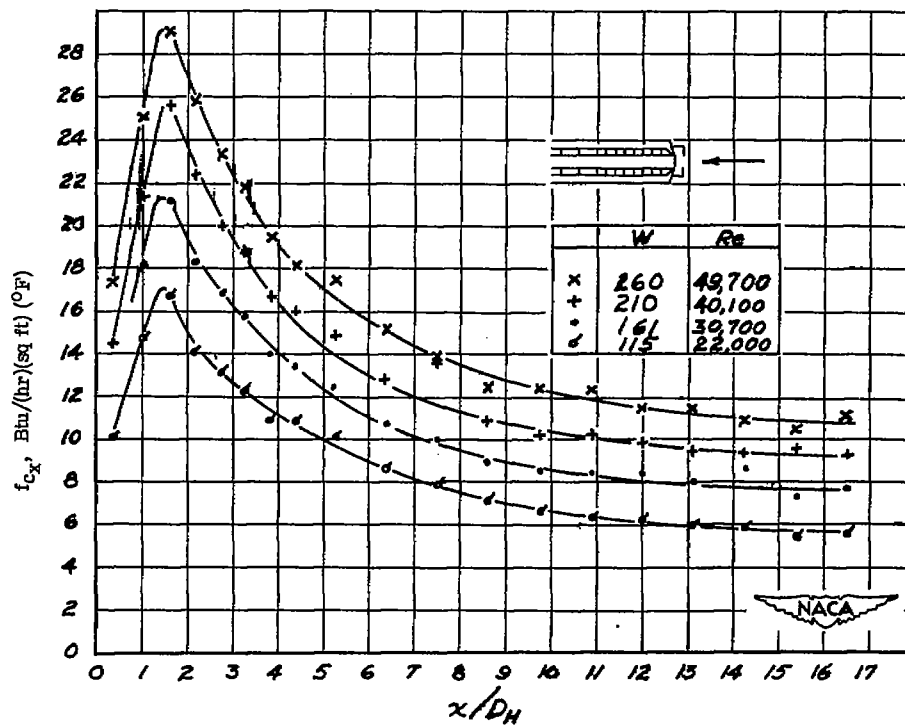
Figure 16.- Variation of point unit thermal conductance in circular tube with large orifice at entrance.
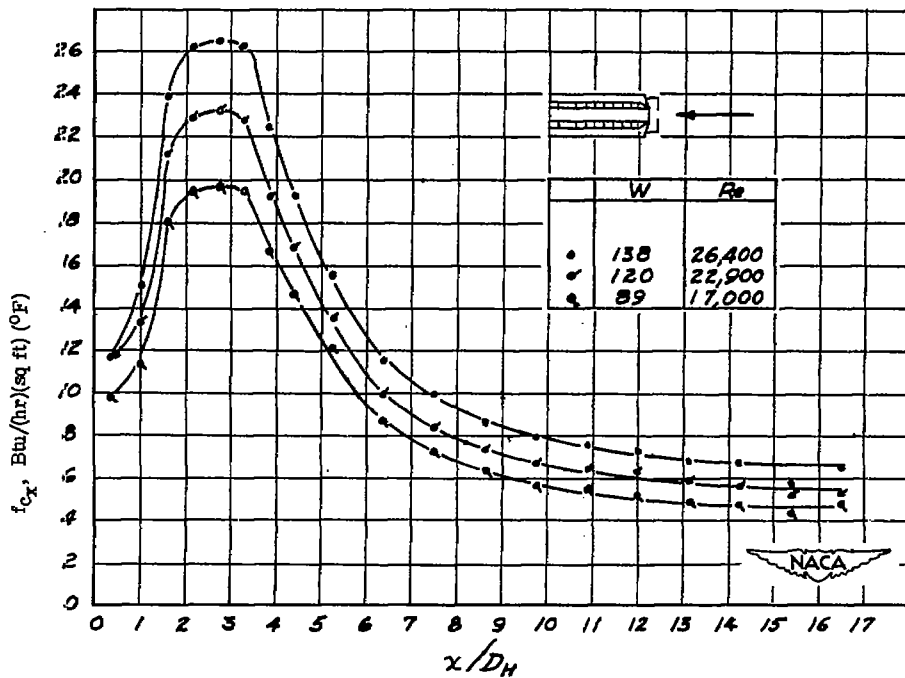


Figure 17.- Variation of point unit thermal conductance in circular tube with small orifice at entrance.
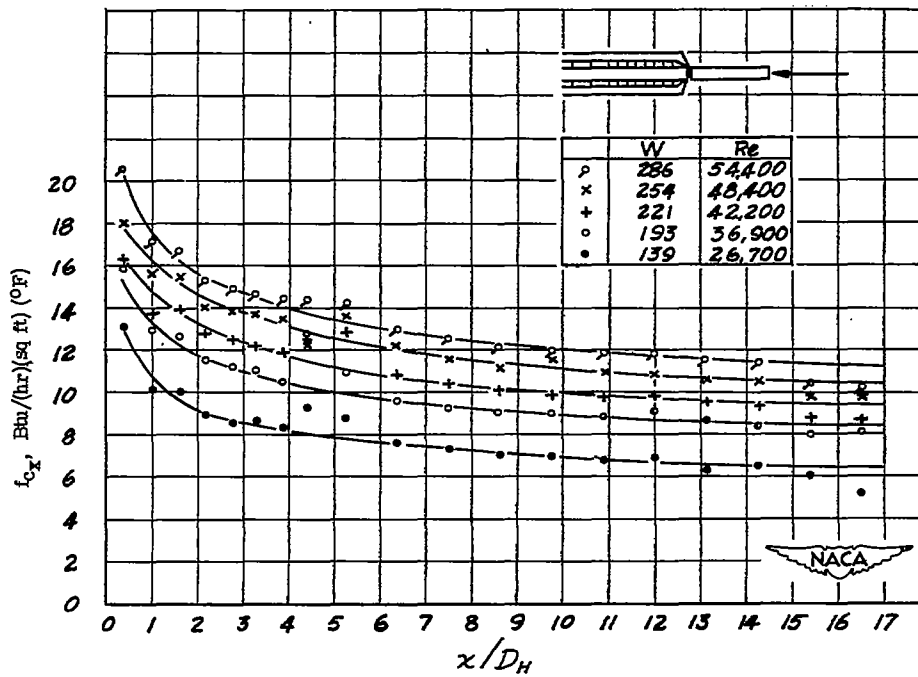
Figure 18.- Variation of point unit thermal conductance in circular tube with short calming section at entrance.
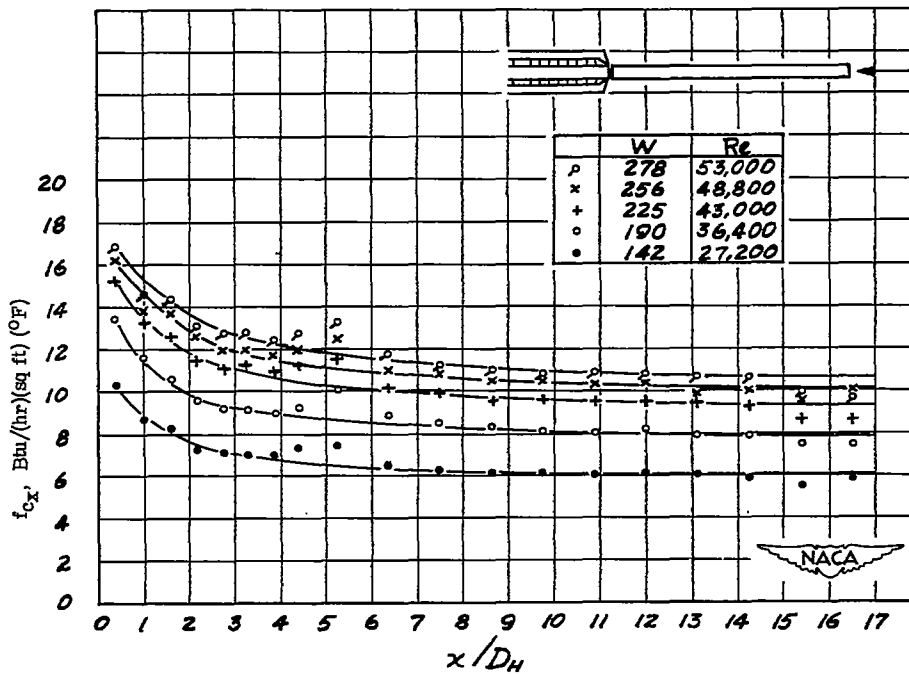


Figure 19.- Variation of point unit thermal conductance in circular tube with long calming section at entrance.
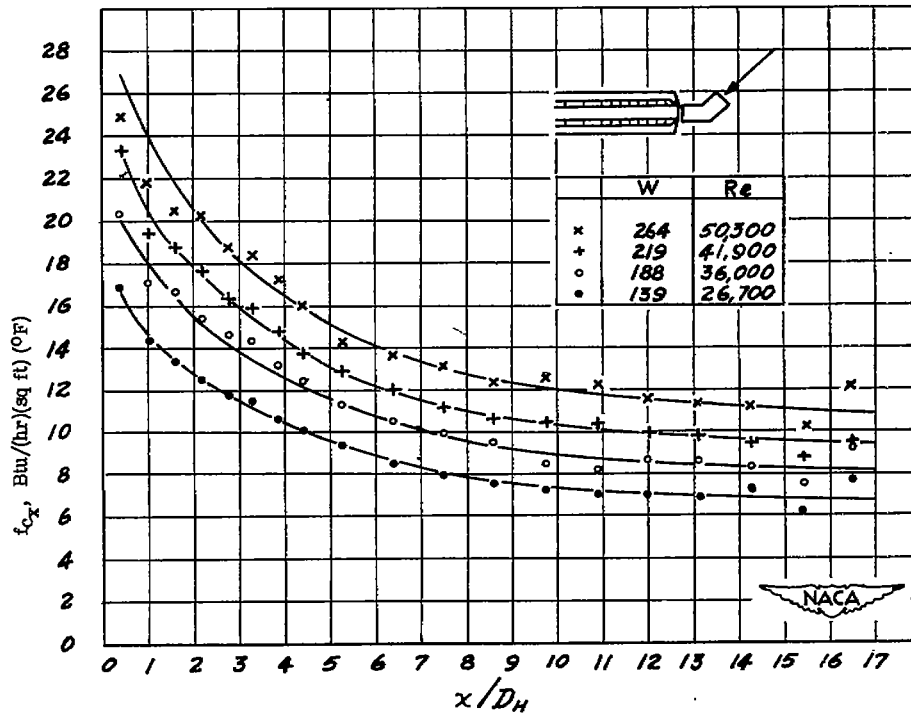
Figure 20.-   Variation of point unit thermal conductance in circular tube with 45°-angle
bend at entrance.
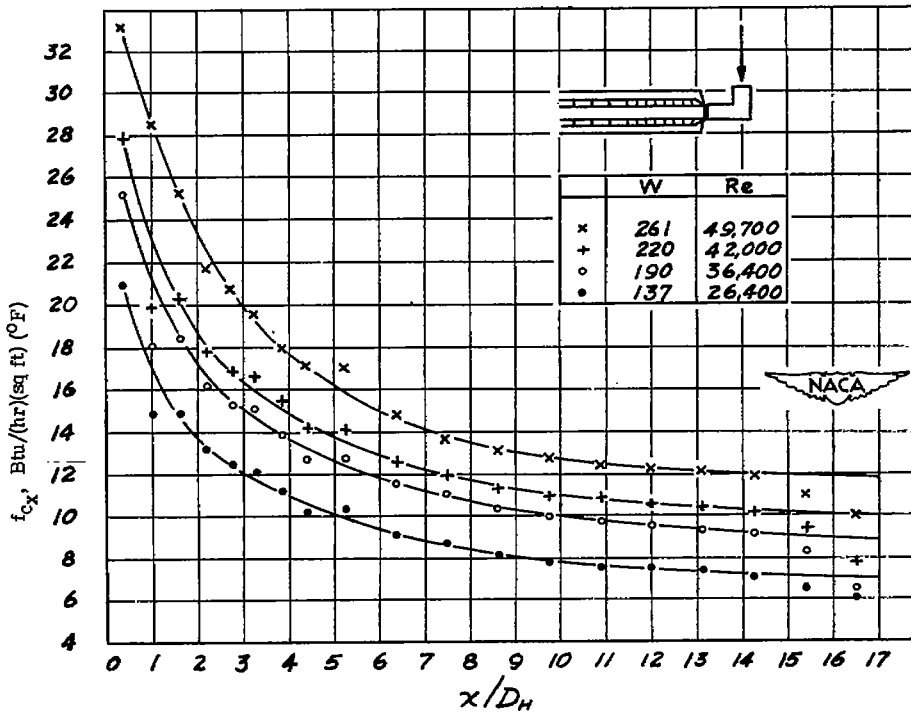


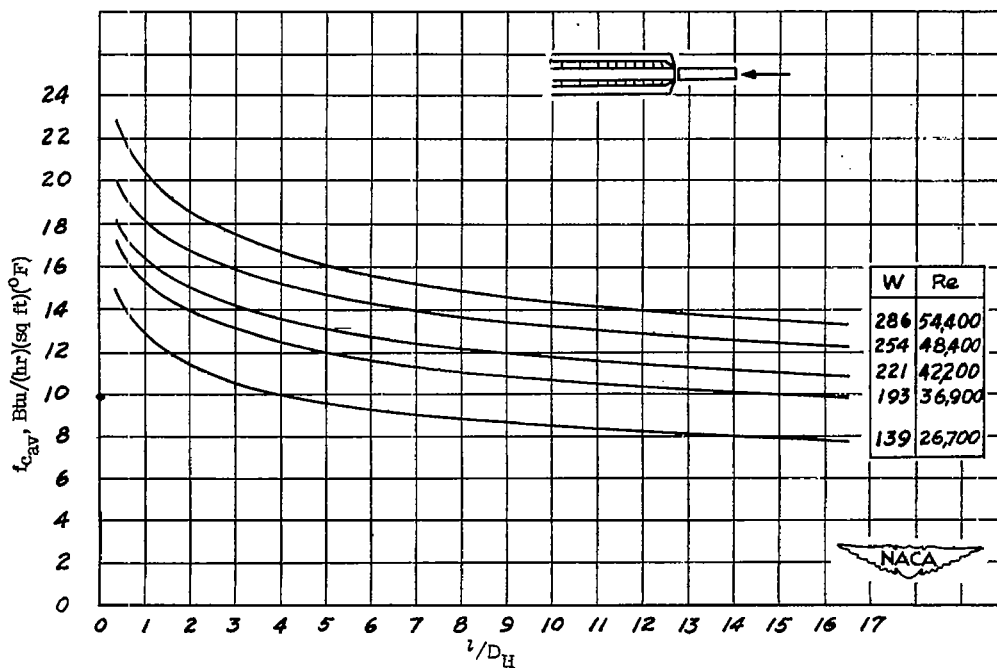Figure 21.-   Variation of point unit thermal conductance in circular tube with right-angle
bend at entrance.
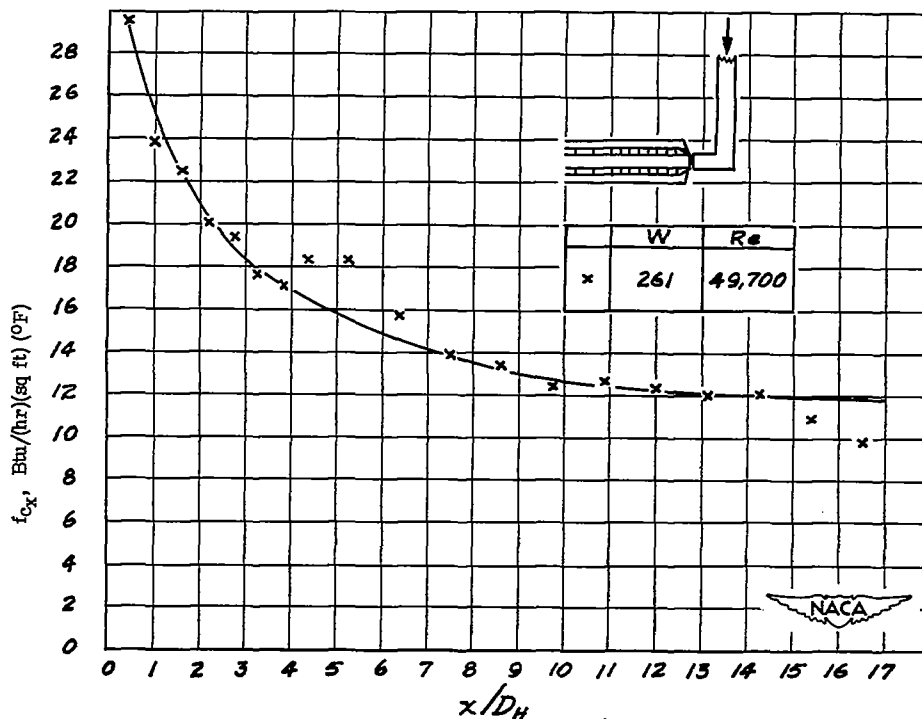
Figure 22.- Variation of point unit thermal conductance in circular tube with right-angle bend and long calming section at entrance.
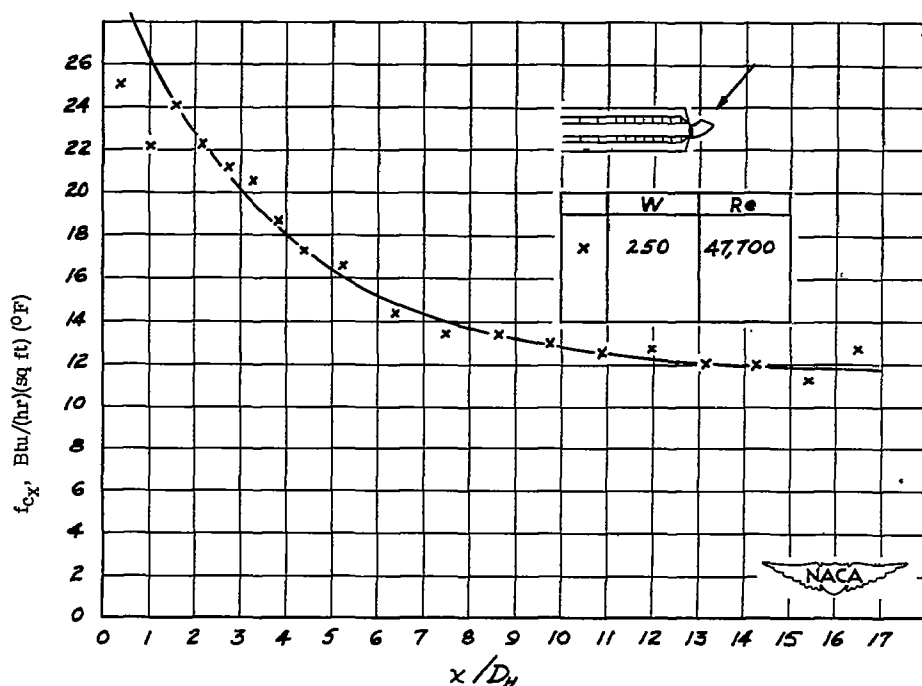
Figure 23.- Variation of point unit thermal conductance in circular tube with 45° round bend at entrance.

Figure 24.-   Variation of point unit thermal conductance in circular tube with 90° round
bend at entrance.
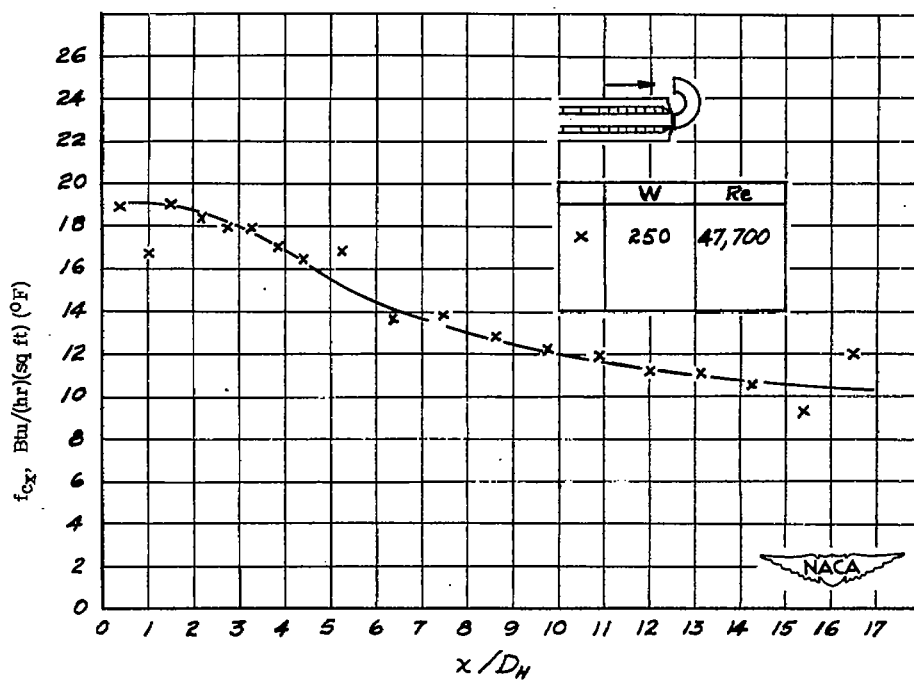


Figure 25.-   Variation of point unit thermal conductance in circular tube with 180° round
bend at entrance.
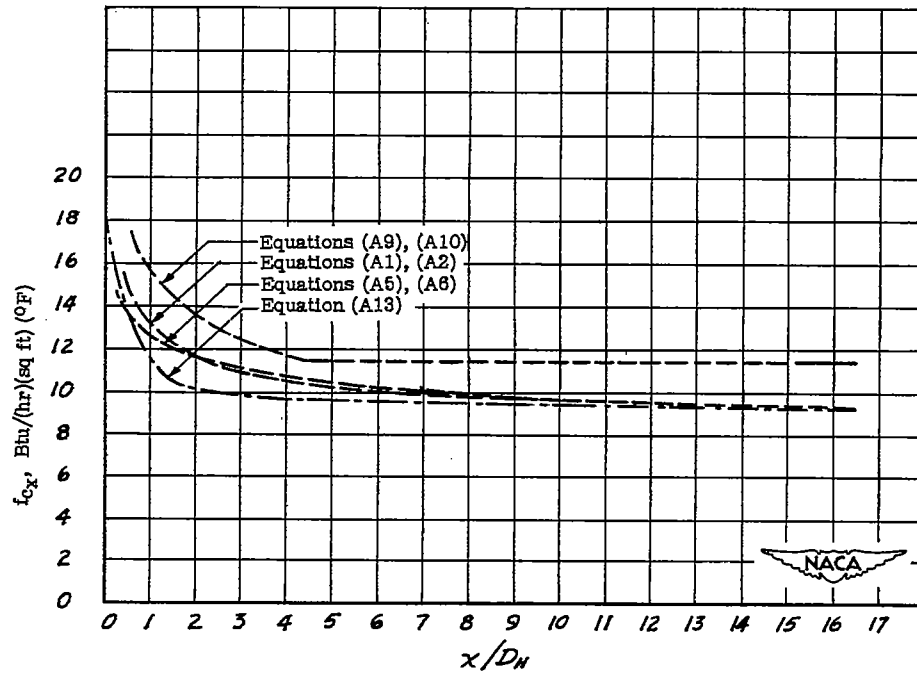
Figure 26.- Comparison of analytical equations for predicting point unit thermal conductance in circular tube.
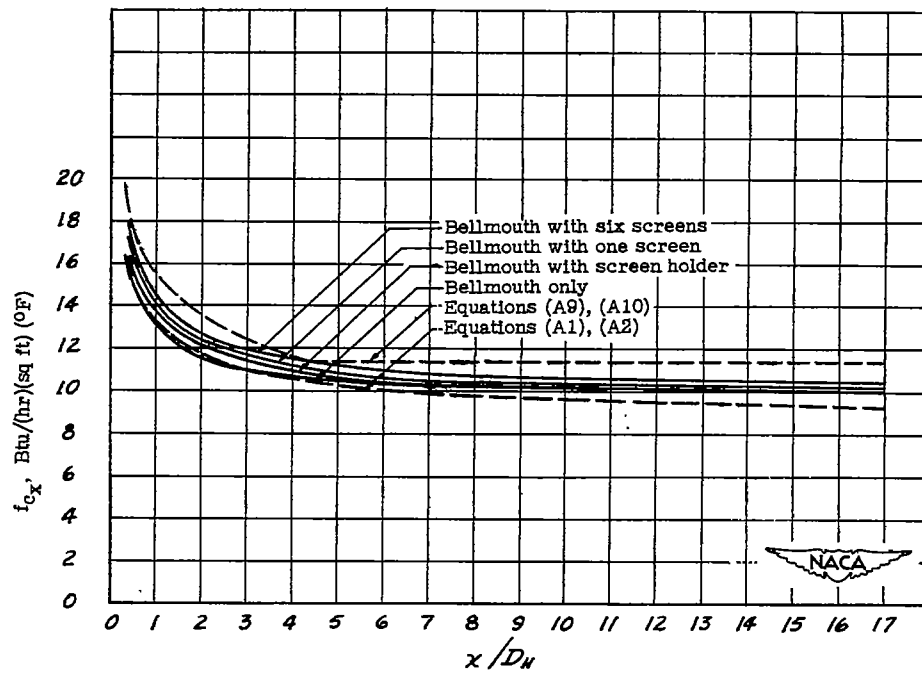


Figure 27.- Comparison of equations (A1), (A2), and (A9), (A10) with experimental data.
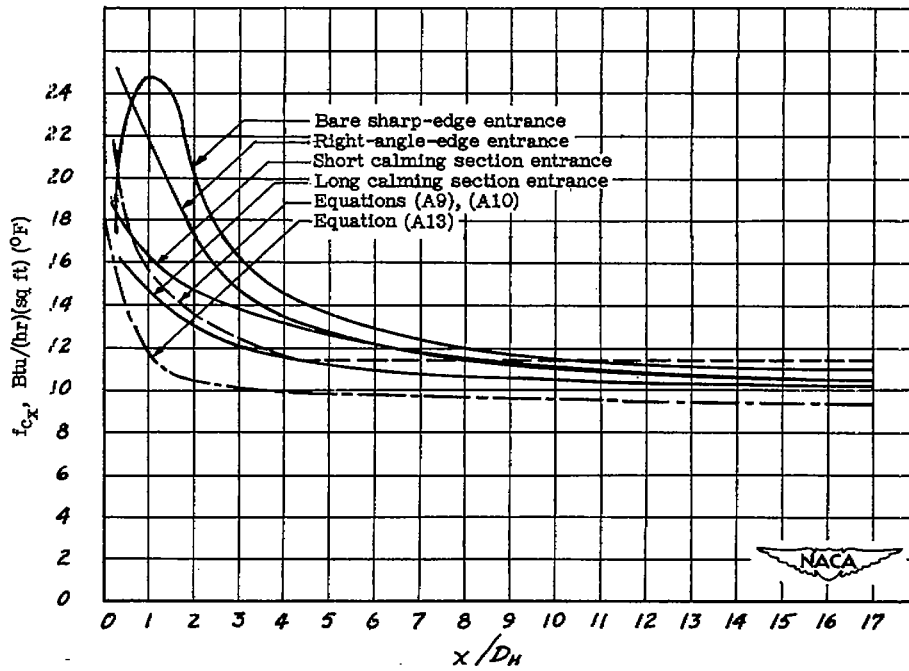
Figure 28.-   Comparison of equations (A9), (A10), and (A13) with
experimental data.
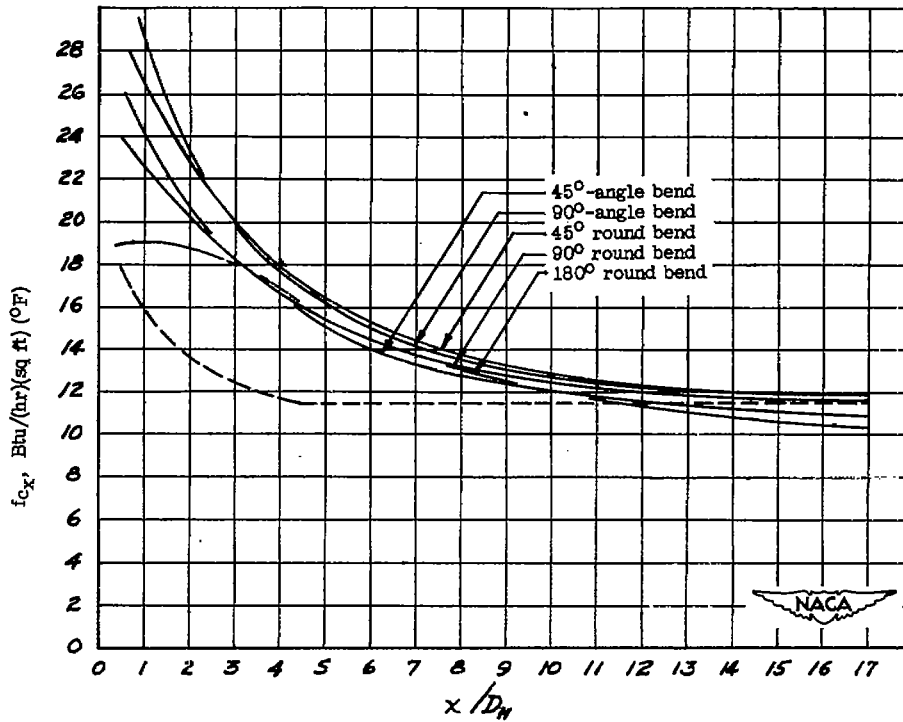


Figure 29.-   Comparison of various bend conditions.
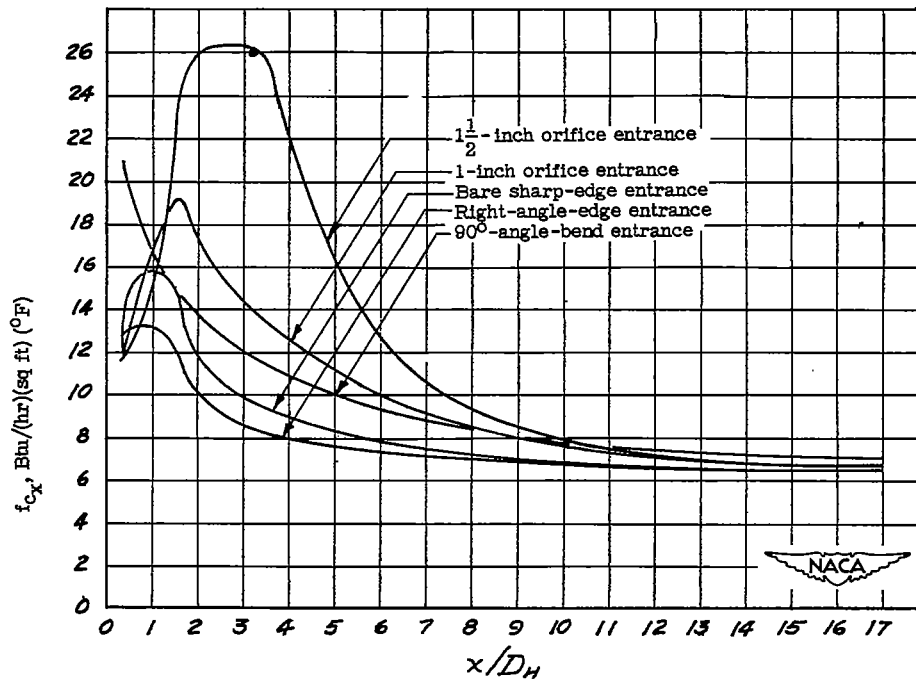
Figure 30.- Comparison of orifice-type-entrance conditions.

Legend on figure:
$1\frac{1}{2}$-inch orifice entrance
1-inch orifice entrance
Bare sharp-edge entrance
Right-angle-edge entrance
$90^{\circ}$-angle-bend entrance

y-axis: $f_{c_x}$, Btu/(hr)(sq ft)($^{\circ}$F)
x-axis: $x/D_H$



| W | Re |
|-----|--------|
| 281 | 53,700 |
| 242 | 46,200 |
| 197 | 37,600 |
| 139 | 26,600 |

y-axis: $f_{c_{av}}$, Btu/(hr)(sq ft)($^{\circ}$F)
x-axis: $l/D_H$
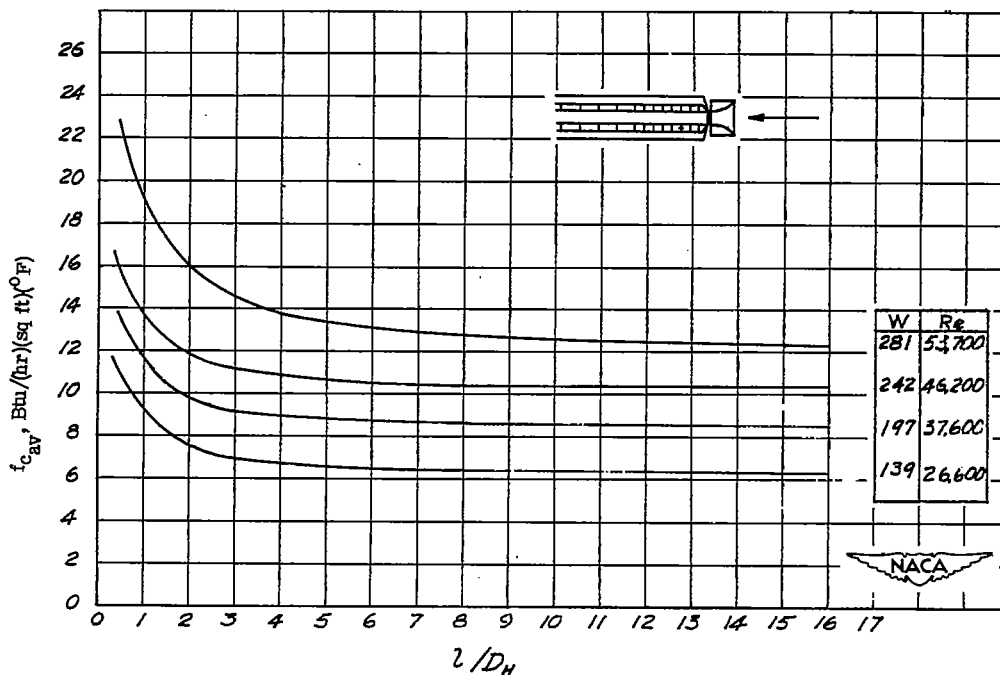
Figure 31.-  Variation of average unit thermal conductance with length in circular tube
with bellmouth.
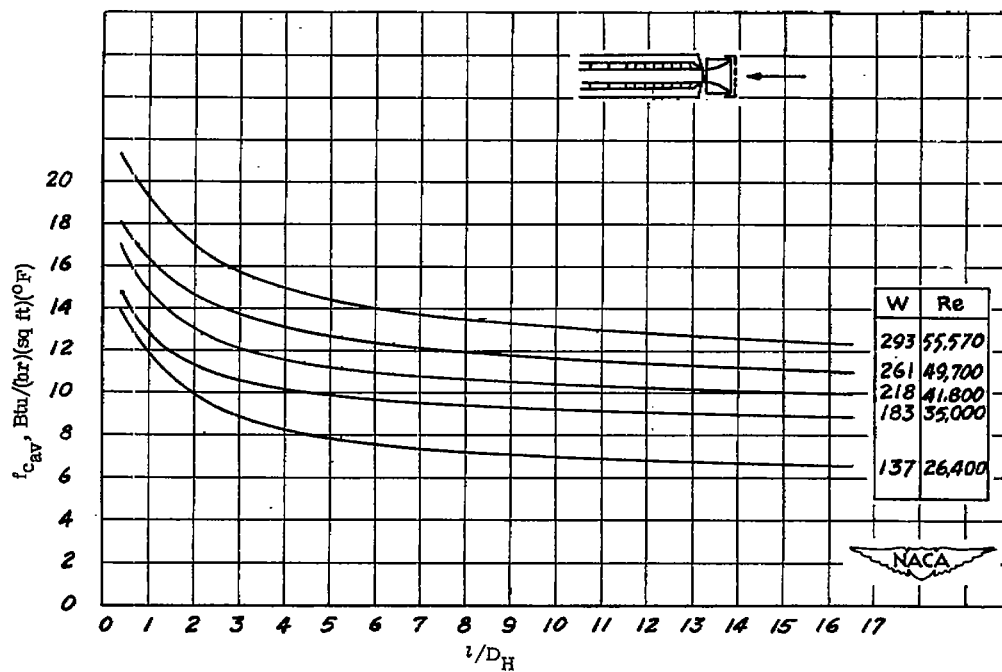
Figure 32.- Variation of average unit thermal conductance with length in circular tube with bellmouth and one screen at entrance.

Figure 33.- Variation of average unit thermal conductance with length in circular tube with short calming section at entrance.
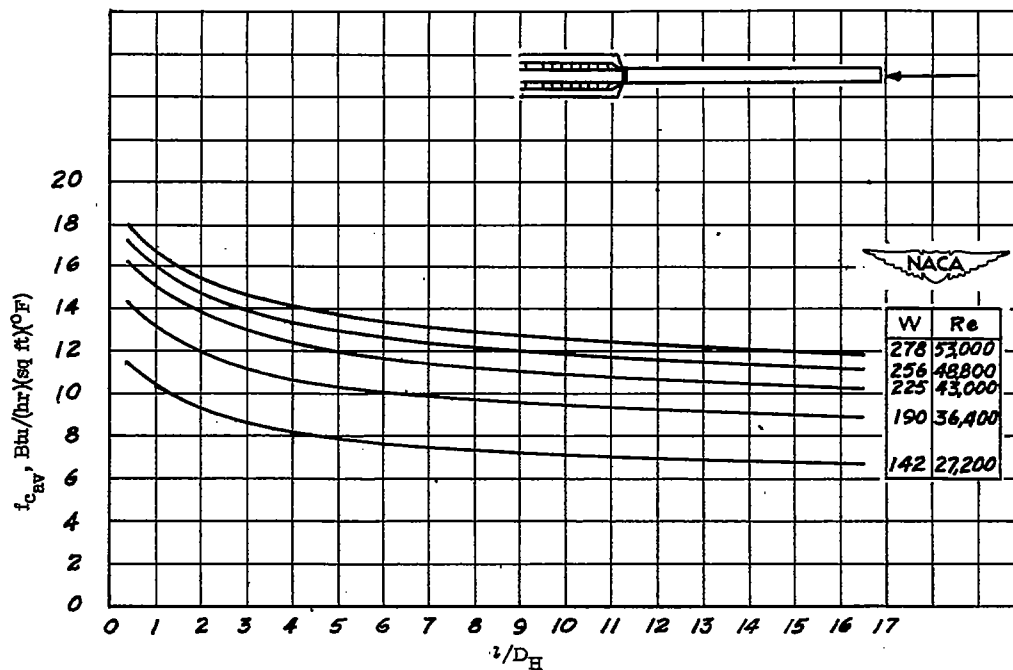
Figure 34.- Variation of average unit thermal conductance with length in circular tube with long calming section at entrance.
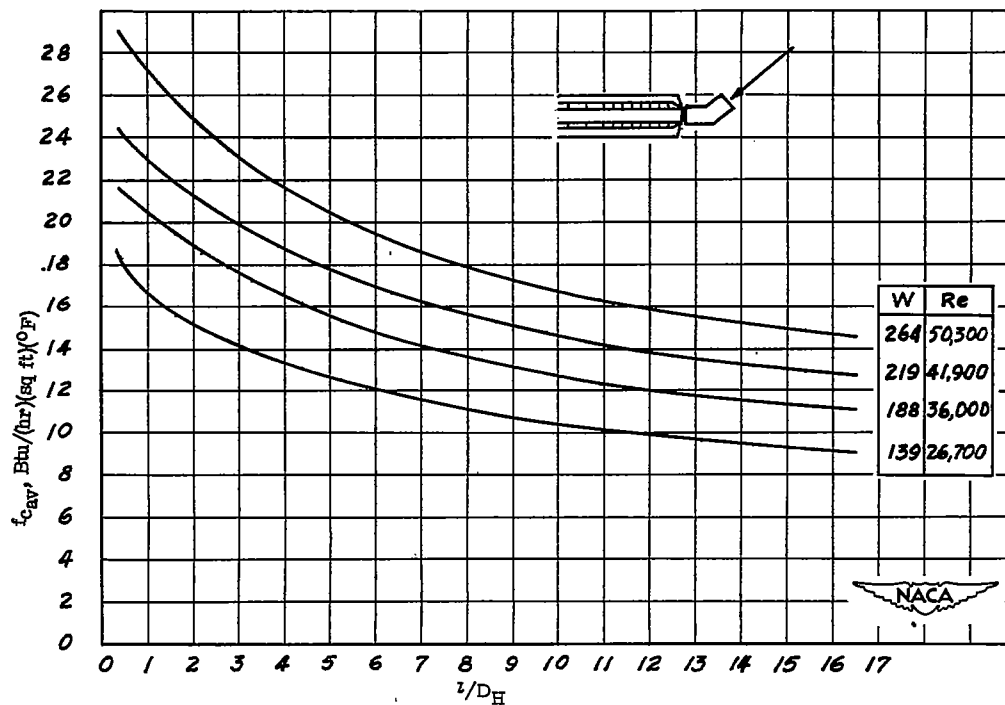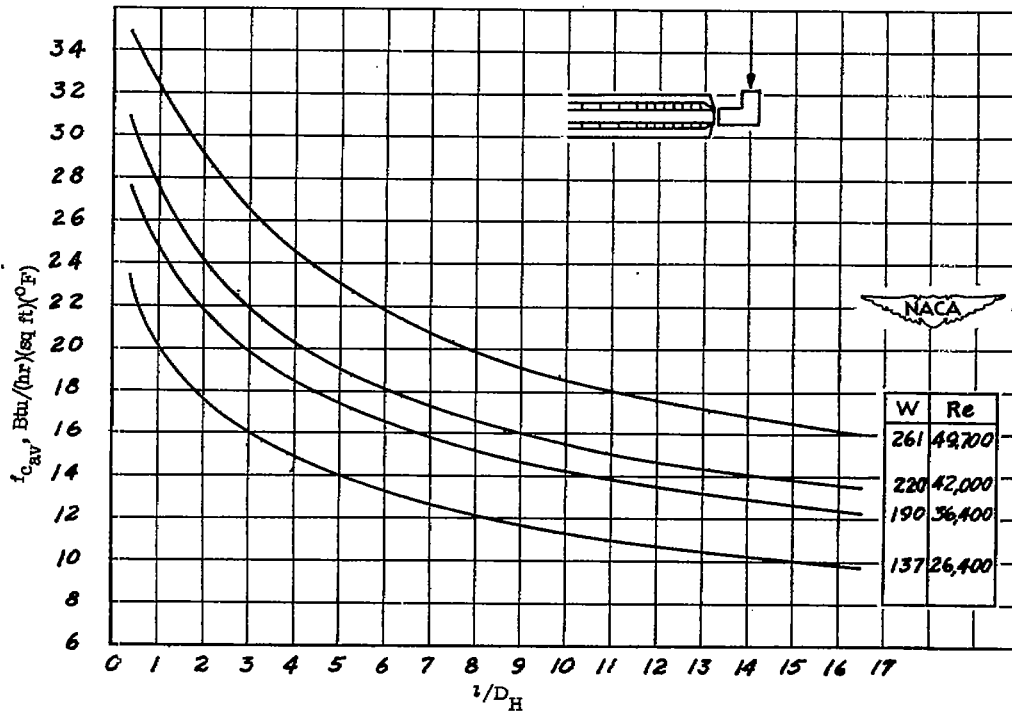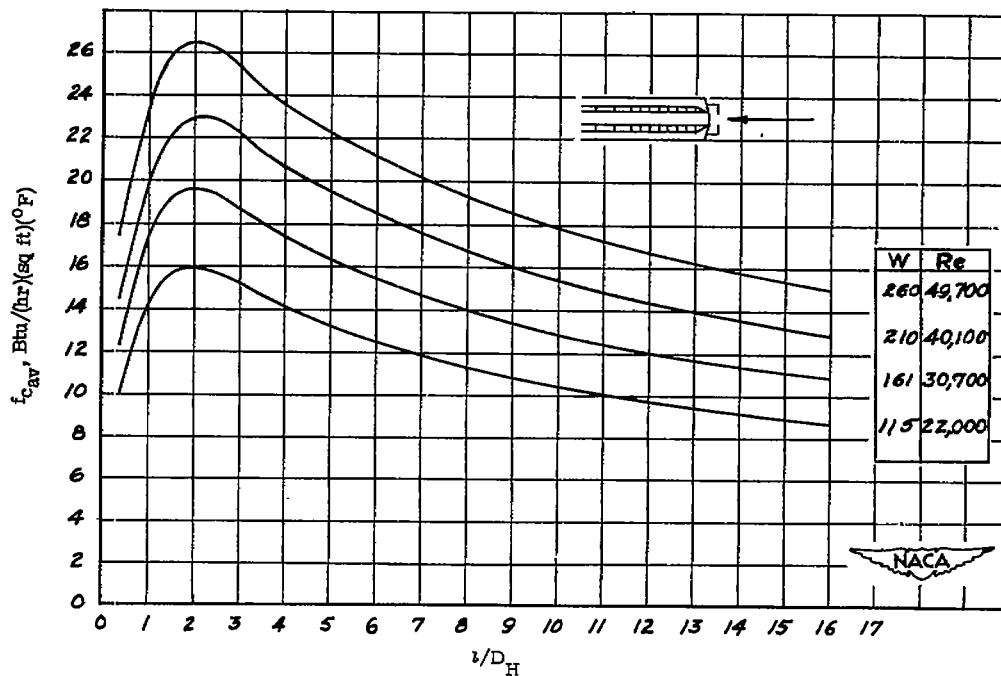


Figure 35.- Variation of average unit thermal conductance with length in circular tube with 45°-angle bend at entrance.

Figure 36.- Variation of average unit thermal conductance with length in circular tube with right-angle bend at entrance.
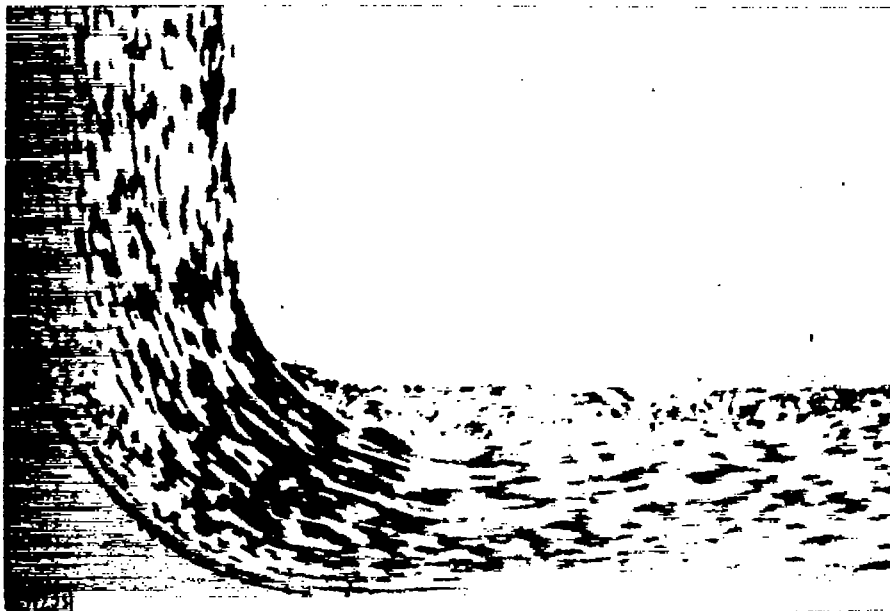


Figure 37.- Variation of average unit thermal conductance with length in circular tube with large orifice at entrance.
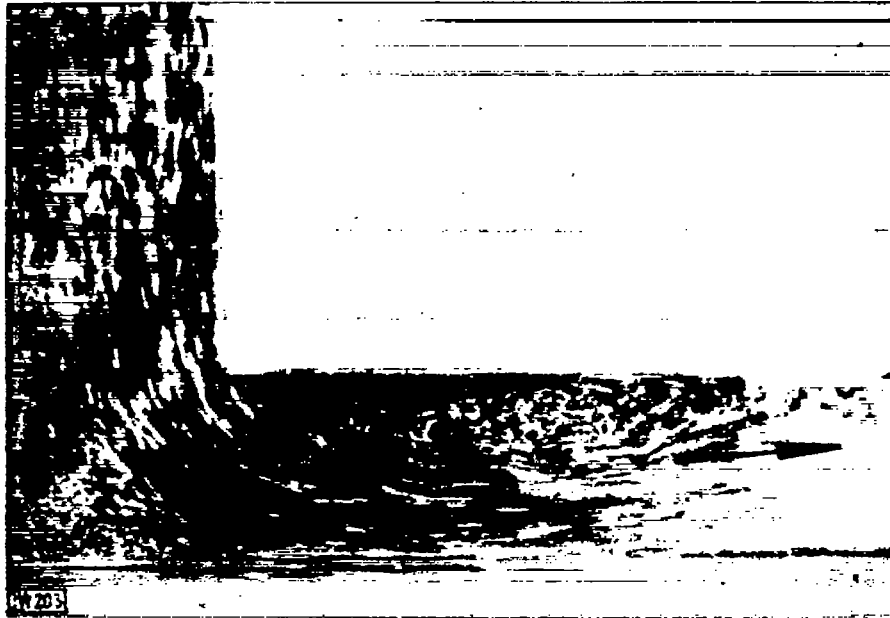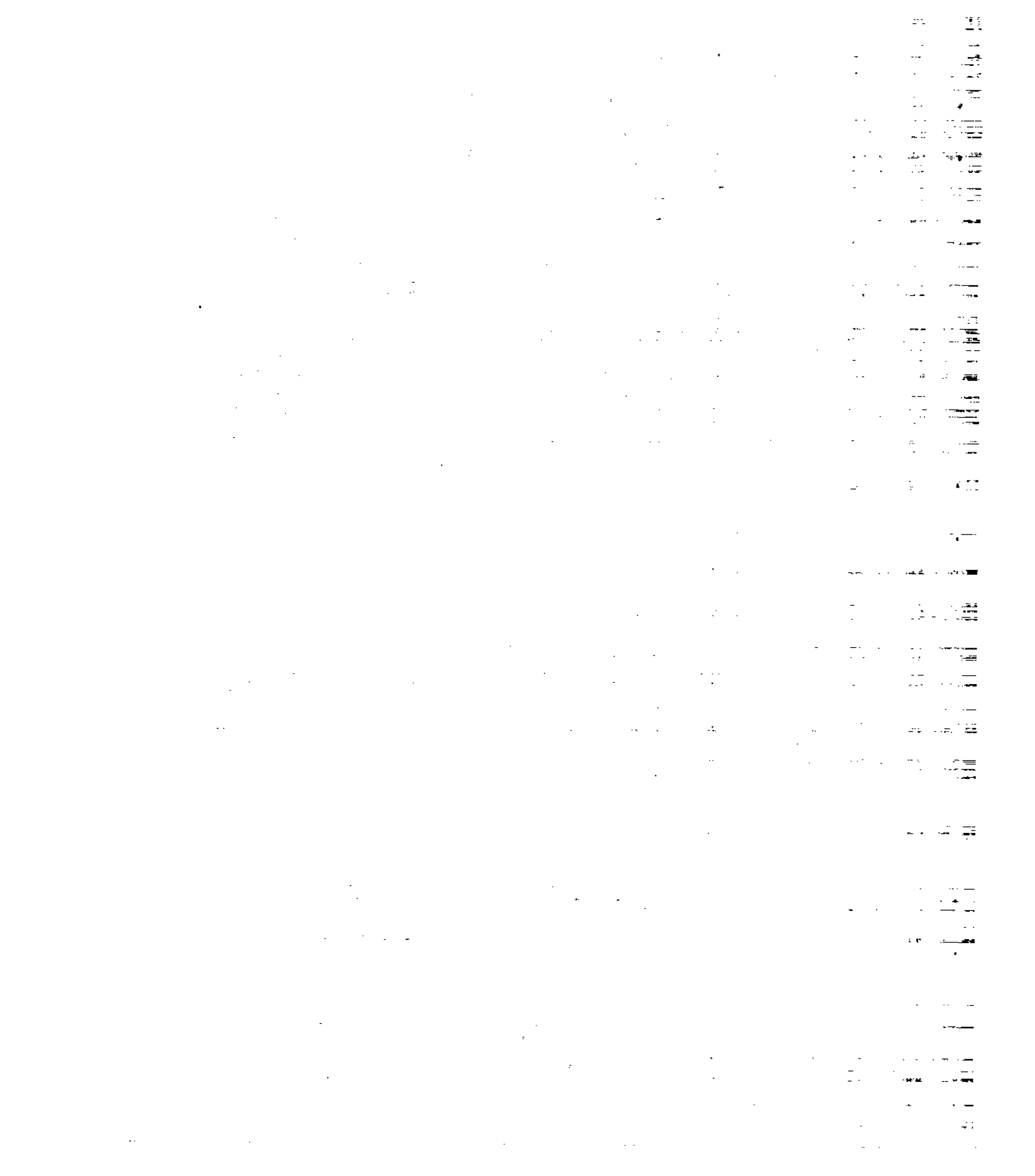
Figure 38.- Photographs showing flow around bends. (Given in "Lärm und Resonanzschwingungen im Kraftwerkstrieb" by Dr. Ing. F. Michel, VDI-Verlag G.m.b.H. (Berlin), 1932.)
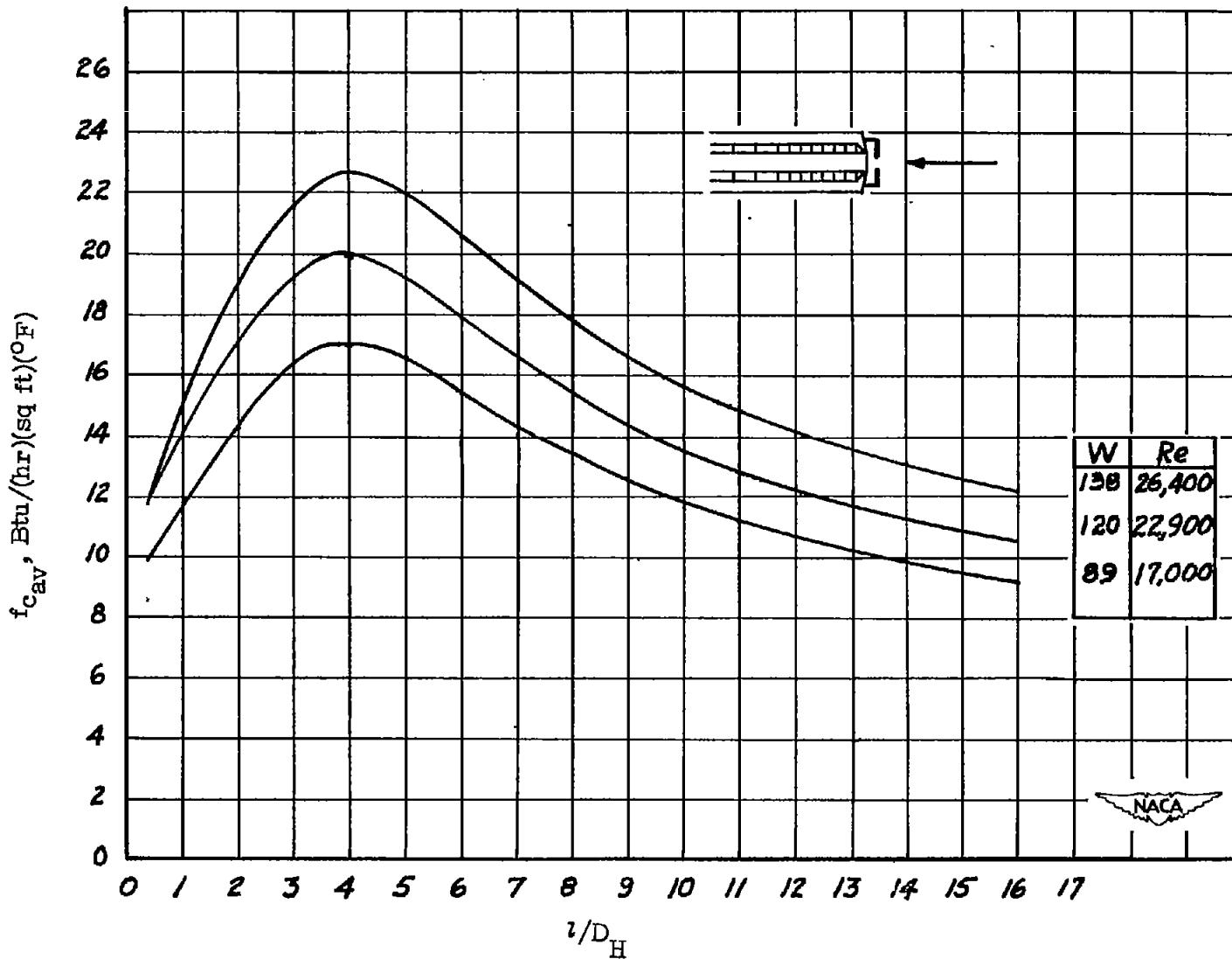
Figure 39.- Variation of average unit thermal conductance with length in circular tube with small orifice at entrance.